Published in *Wave Motion* 118, 2023, #103109
https://doi.org/10.1016/j.wavemoti.2022.103109

Local Absorbing Boundary Conditions for the Elastic Wave Equation

E. Turkel [*] R. Gordon [†] D. Gordon [‡]

Abstract

We compare and analyze absorbing boundary conditions for the elastic wave equations. We concentrate on the first order extensions to Clayton–Enqquist and show the relationship of the Lysmer–Kuhlemeyer ABC to these generalizations. We derive conditions for the reflection coefficient to have the same accuracy for near normal waves as in the acoustic wave case. Extensions to the first order system, spherical coordinates, higher order boundary conditions and frequency domain are derived. We extend Stacey's absorbing boundary condition (ABC) to all six sides of a cubic domain, and show that Stacey's ABC provide good numerical results.

Keywords: Elastic wave equation; Local absorbing boundary conditions; Lysmer–Kuhlemeyer; Stacey's boundary conditions.

1 Introduction

We consider the time dependent elastic equations in an unbounded domain. For computational reasons we need to truncate this to a finite domain. In order to simulate the infinite domain we impose boundary conditions on the far field boundaries so that waves do not reflect back into the domain. Any perfect nonreflecting boundary treatment is non-local in both space and time [12]. Instead, we will consider only local absorbing boundary conditions that minimize the reflections.

For simplicity, as will be explained, we shall consider low order absorbing boundary conditions. We shall see that even in this case the problem is nontrivial. In the acoustic case Engquist and Majda [13] developed a sequence of boundary conditions in Cartesian coordinates. This was based on splitting the wave equation into forward and backward moving waves and eliminating the waves entering the domain. We shall consider the boundary condition on the upper boundary where the domain is $z \le 0, \quad -\infty < x < \infty$. We consider a Cartesian coordinate system with z oriented downward, x parallel with the plane of the paper and y out of the paper. For the two dimensional problem we chose the x-z plane. To change the coordinate system so that z decreases as we descend we replace t by $-t$ in all the formula. The lowest order boundary condition is simply

$$u_t - cu_z = 0 \quad \text{at } z = 0 \tag{1}$$

where c is the speed of sound in the wave equation. This is simply a one dimensional convective equation with the wave moving up (remember z increases as we descend physically), i.e. no waves enter into the domain. For polar coordinates Bayliss and Turkel [4] considered a different approach which introduced

[*]Corresponding author. School of Mathematical Sciences, Tel-Aviv University, Tel-Aviv 6997801, Israel.
Email: turkel@tauex.tau,ac.il
[†]Dept. of Aerospace Engineering, the Technion–Israel Inst. of Technology, Haifa 32000, Israel.
Email: rgordon@technion.ac.il
[‡]Dept. of Computer Science, University of Haifa, Haifa 3498838, Israel. Email: gordon@cs.haifa.ac.il

a lower order term $\frac{u}{2r}$, in two dimensions, into the lowest order ABC. We will analyze extensions of various first and second order local ABCs to the elastic wave equation.

Both approaches (EM and BT) allow for a sequence of higher order absorbing. However, higher order interior methods usually require higher order derivatives in time and space. These can no longer be represented with linear finite elements. With finite differences a larger stencil is required which causes difficulties and frequently demands one sided stencils (see however, [46], [33] for some examples with higher order ABCs for the acoustic equation). Experience with both Engquist-Majda [13] and Bayliss–Turkel [4] for the acoustic wave equation shows that the best low order local schemes are second order.

In recent years several approaches have been presented for higher order absorbing boundary conditions. One of the most popular is the perfectly matched layer (PML) algorithm. This was first developed by Bérenger [7] for Maxwell's equations and later extended to the acoustic wave equation and then the elastic wave equation, see e.g. [22]. (see however, [46], [33] for some examples with higher order ABCs for the acoustic equation). Another approach is to introduce auxiliary variables [38] which increases the size of the system. Other high order approaches include the double absorbing boundary approach [39] and the supergrid approach [3, 35]. However, PML can depend on parameters that are not easy to calculate. Other difficulties of higher order schemes include: some stability issues, implementation for corners of two sets of high-order ABCs, loss of symmetry etc. The higher order schemes generally require more CPU time and storage and hence become competitive only when coupled with a high order interior scheme for high accuracy requirements.

Hence, for many engineering problems low order methods remain very popular. They use a second order finite difference or a linear finite element method coupled with the absorbing boundary scheme of Lysmer and Kuhlemeyer (LK), see, for example, the ABAQUS Theory Manual [1, §3.3.1]. LK has over 3000 citations and is used also in recent papers, e.g. [40, 42]. Thus, while LK is now used more than Clayton–Engquist we shall demonstrate that other lower order but local ABCs have better properties than both these schemes.

2 Elastic Equations

Let $\overrightarrow{u}$ be the velocity vector in the elastic media; so in three dimensions $\overrightarrow{u} = (u, v, w)$. We denote by c_p and c_s the longitudinal and transverse wave speeds, from which the Lamé parameters λ and μ are defined as follows:

$$\lambda = \rho(c_p^2 - 2c_s^2) \quad \text{and} \quad \mu = \rho c_s^2,$$

where ρ is the density in kg/m^3. From this we have

$$c_p = \sqrt{\frac{\lambda + 2\mu}{\rho}} \quad \text{and} \quad c_s = \sqrt{\frac{\mu}{\rho}} \tag{2}$$

In vector form the elastic equations for a homogeneous media are given by

$$\overrightarrow{u}_{tt} = c_p^2 \nabla(\nabla \cdot \overrightarrow{u}) - c_s^2 \nabla \times (\nabla \times \overrightarrow{u}) = (c_p^2 - c_s^2)\nabla(\nabla \cdot \overrightarrow{u}) + c_s^2 \Delta(\overrightarrow{u}) \tag{3}$$

We rewrite (3) in component form

$$\begin{aligned} u_{tt} &= c_p^2 u_{xx} + (c_p^2 - c_s^2)(v_{xy} + w_{xz}) + c_s^2(u_{yy} + u_{zz}) \\ v_{tt} &= c_p^2 v_{yy} + (c_p^2 - c_s^2)(u_{xy} + w_{yz}) + c_s^2(v_{xx} + v_{zz}) \\ w_{tt} &= c_p^2 w_{zz} + (c_p^2 - c_s^2)(u_{xz} + v_{yz}) + c_s^2(w_{xx} + w_{yy}) \end{aligned} \tag{4}$$

The elastic equations, as a time dependent first order system in velocity-stress variables, are given by

$$\rho u_t = \tau_{11x} + \tau_{12y} + \tau_{13z} + F^u(x,y,z,t) \tag{5a}$$
$$\rho v_t = \tau_{12x} + \tau_{22y} + \tau_{23z} + F^v(x,y,z,t) \tag{5b}$$
$$\rho w_t = \tau_{13x} + \tau_{23y} + \tau_{33z} + F^w(x,y,z,t) \tag{5c}$$
$$\tau_{11t} = \rho c_p^2 u_x + \lambda(v_y + w_z) \tag{5d}$$
$$\tau_{22t} = \rho c_p^2 v_y + \lambda(u_x + w_z) \tag{5e}$$
$$\tau_{33t} = \rho c_p^2 w_z + \lambda(u_x + v_y) \tag{5f}$$
$$\tau_{12t} = \rho c_s^2(u_y + v_x) \qquad \rho c_p^2 = \lambda + 2\mu \tag{5g}$$
$$\tau_{13t} = \rho c_s^2(u_z + w_x) \qquad \rho c_s^2 = \mu \tag{5h}$$
$$\tau_{23t} = \rho c_s^2(v_z + w_y) \tag{5i}$$

where F^u, F^v, F^w are the components of the impact force in the x, y, z directions, respectively.

3 Absorbing Boundary Conditions (ABC)

When we extend the ABC from the acoustic wave equation to the elastic wave equation there are two difficulties. First, there is a system of two coupled equations instead of a scalar wave equation. Second, there exists two speeds of propagation c_p and c_s. We note that Maxwell's equations are a coupled set of equations but with only one non-zero speed.

Higdon [25, 26] generalized (1) by eliminating both possible waves. So the lowest order ABC of Higdon is given by

$$(\partial_t - c_p\partial_z)(\partial_t - c_s\partial_z)\overrightarrow{u} = 0. \tag{6}$$

More generally he suggests applying

$$\prod_{j=1}^{j=m}(\beta_j\partial_t - c_p\partial_z) \tag{7}$$

to each component of the solution vector in both two and three space dimensions.

Higdon further writes: The use of c_p in each factor amounts to a normalization of coefficients. The jth operator in (7) is perfectly absorbing for P-waves traveling at angles of incidence $\pm cos^{-1}(\beta_j)$ and S-waves traveling at angles of incidence $\pm cos^{-1}(\frac{\beta_j c_s}{c_p})$, if these angles are real. If $\beta_j < 1$ for all j, then (7) is oriented mainly to P-waves but also helps to absorb S-waves. If the β_js are all near $\frac{c_p}{c_s}$ then this is oriented mainly to S-waves but helps absorb P-waves. For general-purpose use, a compromise is advisable; for example, in the case $m=2$ we could use $\beta_1=1$ and $\beta_2=\frac{c_p}{c_s}$ which is equivalent to (6).

He further claims that applying different boundary operators to different components only gives a small advantage but complicates the stability analysis. These equations have the difficulty that even the lowest order ABC now contains two spatial derivatives and the next ABC will contain a fourth z derivative which makes it very difficult to implement numerically.

An extension of the Engquist-Majda approach to elasticity was developed by Clayton and Engquist [9].

$$\begin{aligned} u_t &= c_s u_z \\ v_t &= c_s v_z \\ w_t &= c_p w_z. \end{aligned} \tag{8}$$

Now the normal and parallel components are treated differently but they are still uncoupled. The second order ABC has coupling in the mixed xz derivative.

Stacey [43] presents an improvement to the first order ABC of Clayton and Engquist which is given by

$$\begin{aligned} u_t &= c_s u_z + (c_p - c_s) w_x \\ v_t &= c_s v_z + (c_p - c_s) w_y \\ w_t &= c_p w_z + (c_p - c_s)(u_x + v_y) \end{aligned} \tag{9}$$

Zhou and Saffari [48] developed absorbing boundary conditions by demanding complete absorption at two incident angles. For one incident angle, θ, in two dimensions, they derived

$$\begin{aligned} u_t &= \frac{1}{\cos(\theta)} \left((c_p \sin^2(\theta) + c_s \cos^2(\theta)) u_z + (c_p - c_s) \sin(\theta) \cos(\theta) w_z \right) \\ w_t &= \frac{1}{\cos(\theta)} \left((c_p - c_s) \sin(\theta) \cos(\theta) u_z + (c_p \cos^2(\theta) + c_s \sin^2(\theta)) w_z \right). \end{aligned} \tag{10}$$

For the incident angle zero they recover the boundary condition of Stacey (9).

Petersson and Sjögreen [34] developed a different variant. This results (note they considered the left boundary) in, using $\frac{\lambda}{\rho} = c_p^2 - 2c_s^2$,

$$\begin{aligned} u_t &= c_s (u_z + w_x) \\ v_t &= c_s (v_z + w_y) \\ w_t &= c_p w_z + \frac{c_p^2 - 2c_s^2}{c_p} (u_x + v_y). \end{aligned} \tag{11}$$

A completely different approach was presented by Lysmer and Kuhlemeyer [32] (note that in their paper u and v are displacements and not velocities; we have changed their equation to account for using u and w as velocities). They introduce the normal and tangential stresses. Their equations become, in 3D,

$$\begin{aligned} \tau_{13} &= \rho c_s u \\ \tau_{23} &= \rho c_s v \\ \tau_{33} &= \rho c_p w \end{aligned} \tag{12}$$

This formula is not derived from any absorbing boundary condition but rather represents a dashpot and is justified by analyzing a plane wave solution. One can also generalize these by considering other coefficients in these equations, e.g. White et el. [47], Kim [28].

If we differentiate these formulae in time and use (5) to eliminate the time derivatives of the stresses eq. (12) is equivalent to eq. (11) We note, that the ABC of Lysmer and Kuhlemeyer, based on a viscous dashpot, is identical to the ABC of Petersson and Sjögreen (11) based on a paraxial equation with an energy minimization. Cohen [10] and Cohen and Jennings [11] use the second order paraxial boundary condition of Clayton–Engquist and present a heuristic analysis why the paraxial approximation is similar to the viscous boundary condition based on the dashpot approach of Lysmer–Kuhlemeyer.

4 Potentials

To reduce the elastic equations to a pair of wave equations, we introduce the Helmholtz decomposition. There exists two potentials, a scalar Φ and a vector Ψ so that

$$\overrightarrow{u} = \nabla \Phi + \nabla \times \Psi \qquad \nabla \cdot \Psi = 0. \tag{13}$$

To invert (13) we multiply by the divergence and curl. Using the identities $\nabla \cdot \nabla \times = 0$, $\nabla \times \nabla = 0$ and $\nabla \times (\nabla \times \Psi) = \nabla(\nabla \cdot \Psi) - \Delta\Psi = -\Delta\Psi$ we get

$$\Delta\Phi = \nabla \cdot \overrightarrow{u} \tag{14a}$$
$$\nabla \times (\nabla \times \Psi) = -\Delta \overrightarrow{u}. \tag{14b}$$

Important note: To find Φ and Ψ from the velocities we need to solve a global relationship.

In two dimensions (x, z) and component form (13) is equivalent to

$$\begin{aligned} u &= \Phi_x - \Psi_{2z} \\ w &= \Phi_z + \Psi_{2x}. \end{aligned} \tag{15}$$

Since the only component of Ψ that enters is the normal to the plane, Ψ_2 we will drop the subscript 2.

The potentials solve

$$\begin{aligned} \Phi_{tt} &= c_p^2 \Delta\Phi \\ \Psi_{tt} &= c_s^2 \Delta\Psi. \end{aligned} \tag{16}$$

Randall [41] suggests solving the wave equations for the potentials and the using (15) to find the velocities. They use an absorbing boundary of Lindman [31] for the wave equation. This approach assumes that initial and boundary conditions for the elastic equation can be given in terms of the potentials.

To do some analysis we expand the potentials in terms of plane waves. For simplicity we define the following exponentials

$$\begin{aligned} E_1 &= e^{ik_p(x\sin(\theta)+z\cos(\theta))+i\omega t} \\ E_2 &= e^{ik_p(x\sin(\theta)-z\cos(\theta))+i\omega t} \\ E_3 &= e^{ik_s(x\sin(\phi)-z\cos(\phi))+i\omega t} \end{aligned} \tag{17}$$

Note, that at the boundary $z = 0$ we have $E_1 = E_2 = e^{ik_p sin(\theta)x - i\omega t}$ and $E_3 = e^{ik_s \sin(\phi)x - i\omega t}$. However, we have

$$\omega = c_p k_p = c_s k_s \tag{18a}$$
$$k_p \sin(\theta) = k_s \sin(\phi) \qquad \text{or } c_s \sin(\theta) = c_p \sin(\phi) \tag{18b}$$

and so $E_3 = E_1 = E_2$ at $z = 0$.

Following Achenbach [2], Lysmer–Kuhlemeyer [32], Peterson et al. [34] and D. Rabinovich et al. [38] we consider an incident P wave and a reflected P and S wave. So

$$\begin{aligned} \Phi &= E_1 + R_{PP}E_2 \\ \Psi &= R_{PS}E_3 \end{aligned} \tag{19}$$

Note, that we are expressing the potentials in terms of plane waves. Other researchers have expressed the displacements or velocities in terms of plane waves. Since the potentials solve a wave equation we felt it was more appropriate to use (19). It then follows from (15) that

$$\begin{aligned} u &= ik_p \sin(\theta)(E_1 + R_{PP}E_2) + ik_s R_{PS} \cos(\phi) E_3 \\ w &= ik_p \cos(\theta)(E_1 - R_{PP}E_2) + ik_s R_{PS} \sin(\phi) E_3 \end{aligned} \tag{20}$$

Since all the E_i are equal at $z = 0$ we can divide by them and so equivalently set them equal to one.

We note that in two dimensions (9) and (11) can be written as:

$$\begin{aligned} u_t &= c_s u_z + \beta w_x \\ w_t &= c_p w_z + \alpha u_x. \end{aligned} \tag{21}$$

Define:

$$M = c_p \cos^2(\theta) + \alpha \sin^2(\theta) = c_p - (c_p - \alpha)\sin^2(\theta) \tag{22a}$$

$$\begin{aligned} N &= c_s \cos^2(\phi) - \beta \sin^2(\phi) = c_s - (c_s + \beta)\sin^2(\phi) \\ &= c_s - \frac{c_s^2}{c_p^2}(c_s + \beta)\sin^2(\theta) \quad \text{by (18b)} \end{aligned} \tag{22b}$$

As a reminder:

Clayton–Engquist $\alpha = \beta = 0$ so $M = c_p cos^2(\theta)$ $N = c_s \cos^2(\phi) = c_s(1 - \frac{c_s^2}{c_p^2}\sin^2(\theta))$

Stacey $\alpha = \beta = c_p - c_s$ so $M = c_p - c_s \sin^2(\theta)$ $N = c_s - c_p \sin^2(\phi) = c_s(1 - \frac{c_s}{c_p})\sin^2(\theta)$

Petersson–Sjögreen $\alpha = c_p - \frac{c_s^2}{c_p}, \beta = c_s$ so $M = c_p - \frac{c_s^2}{c_p}\sin^2(\theta)$,

$$N = c_s(1 - 2\sin^2(\phi)) = c_s(1 - 2\frac{c_s^2}{c_p^2}\sin^2(\theta)).$$

We differentiate (20) and substitute into (21). This yields, in 2D,

$$\begin{aligned} 0 &= -u_t + c_s u_z + \beta w_x = \omega k_p \sin(\theta) - k_p^2(c_s + \beta)\sin(\theta)\cos(\theta) \\ &\quad + \left(\omega k_p \sin(\theta) + k_p^2(c_s + \beta)\sin(\theta)\cos(\theta)\right) R_{PP} \\ &\quad + \left(\omega k_s \cos(\phi) + k_s^2 N\right) R_{PS} \\ 0 &= -w_t + c_p w_z + \alpha u_x = \omega k_p \cos(\theta) - k_p^2 M \\ &\quad - \left(\omega k_p \cos(\theta) + k_p^2 M\right) R_{PP} \\ &\quad + \left(\omega k_s \sin(\phi) + k_s^2(c_p - \alpha)\sin(\phi)\cos(\phi)\right) R_{PS} \end{aligned} \tag{23}$$

We have two equations for R_{PP} and R_{PS} where α and β are parameters to be chosen. θ and ϕ are the angles of incidence and the reflection angle of the S wave. We next solve the two equations for the two unknown reflection amplitudes. Then

$$\begin{aligned} det &= k_p k_s \left\{\omega^2 \left(\sin(\theta)\sin(\phi) + \cos(\theta)\cos(\phi)\right)\right. \\ &+ \omega \cos(\theta)\left(k_s N + k_p(\beta + c_s)\sin(\theta)\sin(\phi)\right) \\ &+ \omega \cos(\phi)\left(k_p M + k_s(c_p - \alpha)\sin(\theta)\sin(\phi)\right) \\ &+ \left. k_p k_s \left((c_p - \alpha)(\beta + c_s)\sin(\theta)\sin(\phi)\cos(\theta)\cos(\phi) + MN\right)\right\} \\ R_{PP} &= k_p k_s \left\{\omega^2 \left(\cos(\theta)\cos(\phi) - \sin(\theta)\sin(\phi)\right)\right. \\ &+ \omega \left(\cos(\theta)(k_s N + k_p(\beta + c_s)\sin(\theta)\sin(\phi)\right) \\ &- \cos(\phi)(k_p M + k_s(c_p - \alpha))\sin(\theta)\sin(\phi) \\ &+ \left. k_p k_s \left((c_p - \alpha)(\beta + c_s)\sin(\theta)\sin(\phi)\cos(\theta)\cos(\phi) - MN\right)\right\} / det \\ R_{PS} &= -2k_p^2 \sin(\theta)\cos(\theta)\left(\omega^2 - k_p^2(\beta + c_s)M\right) / det \end{aligned} \tag{24}$$

Lemma 1. *If* $0 < \alpha \leq c_p$ *and* $-c_s \leq \beta \leq 2(c_p - c_s)$ *then det is positive and* $|R_{PP}| \leq 1$.

Proof. We wish all the individual terms to be positive. Then the result for $|R_{PP}|$ follows by the triangle inequality. So we require that $c_p-\alpha$, $\beta+c_s$,M,N all be positive. M is positive if $\alpha>0$ and so we need N to be positive. All the various sines and cosines are all positive and so the result follows.

It only remains to find the condition for $N \geq 0$. We examine (22b). The angle ϕ is the reflection angle which we cannot control and so we have expressed N also in terms of θ. Since θ is arbitrary between $(0, \frac{\pi}{2})$ we require that $\beta \leq \frac{c_p^2}{c_s} - c_s = \frac{c_p^2 - c_s^2}{c_s} = (c_p - c_s)\frac{c_p + c_s}{c_s}$. So a sufficient condition for N to be positive is $\beta \leq (c_p - c_s)(1 + \frac{c_p}{c_s})$. Since, $c_s \leq c_p$ a sufficient condition for N to be positive is $\beta \leq 2(c_p - c_s)$.

Lemma 2. *We consider angles close to normal, i.e $\theta << 1$. Then $|R_{PP}| = O(\theta^2)$ and $|R_{PS}| = O(\theta)$. For the Stacey formula $|R_{PS}| = O(\theta^3)$.*

Proof. For small θ and ϕ we have $M = c_p, N = c_s$ with an error of $O(\theta^2)$. So by inspection $det = k_p k_s\{\omega^2 + \omega(k_p c_p + k_s c_s) + k_p c_p k_s c_s\}$. But $\omega = k_s c_s = k_p c_p$ and so $det = (\omega + k_p c_p)^2 + O(\theta^2)$. By a similar argument $R_{pp} = \frac{k_p k_s}{det}(\omega^2 - k_p^2 c_p^2 + O(\theta^2)) = O(\theta^2)$. However, for general β R_{PS} is only $O(\theta)$. To increase the accuracy we need $\beta + c_s = c_p + O(\theta)$ or $\beta = c_p - c_s$ which is the formula of Stacey. At this point there is no limitation on α. However, by considering an incoming S wave we require $\alpha = c_p - c_s$. Hence, we have shown that if we consider the general formula (21) (which includes LK) the only formula that has reflections of the order of $O(\theta^2)$ is that of Stacey.

So for the Stacey scheme we have $\sin(\phi) = \frac{c_s}{c_p}\sin(\theta)$, $\cos(\phi) = \sqrt{1 - \sin^2(\phi)}$.

$$
\begin{aligned}
&\frac{det}{\omega^2 k_p k_s} = \sin(\theta)\sin(\phi) + \cos(\theta)\cos(\phi) \\
&+ (\cos(\theta)+\cos(\phi))(1+\sin(\theta)\sin(\phi)) - \frac{c_p}{c_s}\cos(\theta)\sin^2(\phi) - \frac{c_s}{c_p}\cos(\phi)\sin^2(\theta) \\
&+ \sin(\theta)\sin(\phi)\cos(\theta)\cos(\phi) + 1 - \frac{c_p}{c_s}\sin^2(\phi) - \frac{c_s}{c_p}\sin^2(\theta) + \sin^2(\theta)\sin^2(\phi) \\
&|R_{PP}| = \{sin(\theta)\sin(\phi) - \cos(\theta)\cos(\phi) \\
&+ (\cos(\theta) - \cos(\phi))(1+\sin(\theta)\sin(\phi)) - \frac{c_p}{c_s}\cos(\theta)\sin^2(\phi) + \frac{c_s}{c_p}\cos(\phi)\sin^2(\theta) \\
&+ \sin(\theta)\sin(\phi)\cos(\theta)\cos(\phi) - 1 + \frac{c_p}{c_s}\sin^2(\phi) + \frac{c_s}{c_p}\sin^2(\theta) - \sin^2(\theta)\sin^2(\phi)\Big\} \\
&/ \frac{det}{\omega^2 k_p k_s} \\
&|R_{PS}| = 2\frac{k_p^4 c_p c_s}{\omega^2 k_p k_s}\sin^3(\theta)\cos(\theta) / \frac{det}{\omega^2 k_p k_s} \qquad (25) \\
&= 2\frac{k_p}{k_s}\frac{c_s}{c_p}\sin^3(\theta)\cos(\theta) / \frac{det}{\omega^2 k_p k_s} \\
&= 2\frac{c_s^2}{c_p^2}\sin^3(\theta)\cos(\theta) / \frac{det}{\omega^2 k_p k_s}
\end{aligned}
$$

The term $\omega^2 k_p k_s$ cancels between the numerator and denominator. The remaining expression for $|R_{PS}|$ depends only on $\sin(\theta)$ and the ratio $\frac{c_s}{c_p}$. We can no longer determine analytically the conditions on $\frac{c_s}{c_p}$ so that $|R_{PS}| \leq 1$. We calculate numerically both $|R_{PS}|$ and $|R_{PS}|$. In figure 1 we plot the maximum over all incident angles as a function of $\frac{cs}{cp}$. In the top figure the maximum is close to zero for a ratio less than 0.7 and so hard to see in the figure. This shows that the reflection coefficient for both the reflected P and S waves are less than 1 for all ratios of c_s to c_p. We note that $\frac{c_s}{c_p} = \sqrt{\frac{\mu}{\lambda+2\mu}} = \sqrt{\frac{1}{2+\lambda/\mu}} \leq \sqrt{\frac{1}{2}} \approx .717$. For most media $\frac{c_s}{c_p} \approx .5$. Hence, for a P wave impinging on the absorbing boundary the reflected P wave has an amplitude close to zero and the reflected S wave has an amplitude of about 10% of the incoming wave.

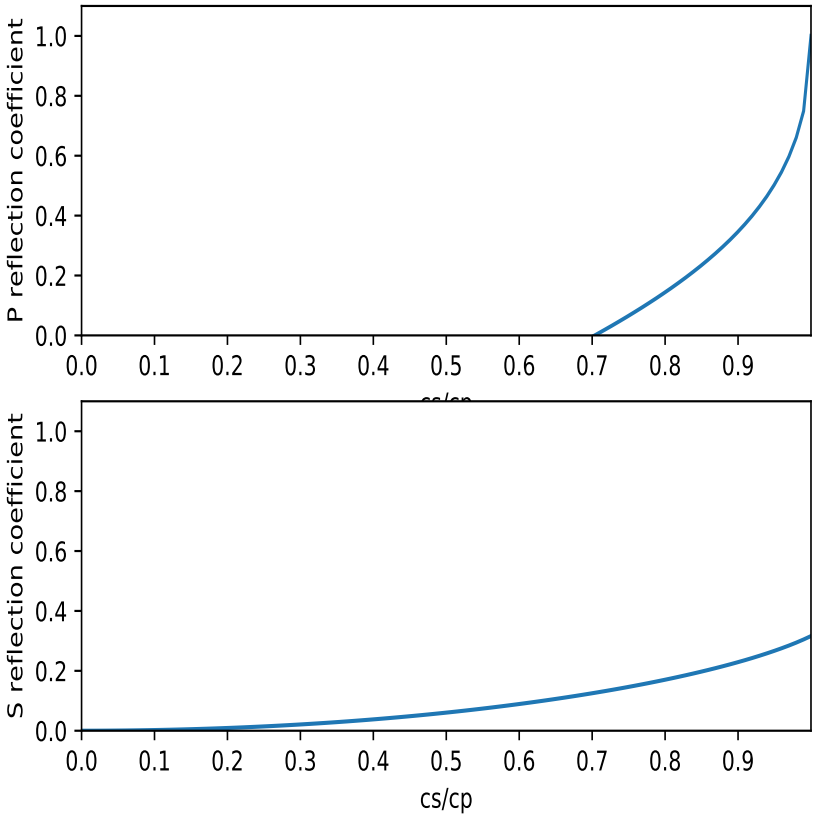

Figure 1: top plot of $|R_{PP}|$, bottom plot R_{PS} as a function of $\frac{c_s}{c_p}$.

Engquist and Majda [13] showed that for their first order ABC, for the acoustic wave equation, one has (changing to our notation) for the reflected wave

$$R = \left(\frac{\cos(\theta) - 1}{\cos(\theta) + 1} \right) \approx \theta^2 \tag{26}$$

where θ is the angle of incidence normal to the top surface.

Clayton–Engquist ignores terms like $\sin(\theta)\cos(\theta)$ while Stacey ignores terms that behave like $\sin^3(\theta)$. In both cases for a wave impinging normal on the boundary $\theta = 0$ the two formulae have no error with respect to the first order wave equation ABC which itself has no error. For waves that are close to normal, $\sin(\theta) << 1$, the extra error in the Stacey formula is small compared to the first order error already existing in Engquist-Majda (26) (θ^2). However, the extra error in the Clayton–Engquist, Petersson–Sjögreen and hence Lysmer–Kuhlemeyer are larger than the first order error already existing in the Engquist-Majda ABC.

5 Spherical Coordinates

We next extend the previous results to spherical coordinates. From [4] we know that even for the acoustic case there is a difference between two and three space dimensions. We shall only consider the 3D case.

The spherical coordinates are defined by

$$\begin{aligned} r^2 &= x^2 + y^2 + z^2 \\ \tan(\theta) &= \frac{y}{x} \\ \cos(\phi) &= \frac{z}{r} \end{aligned} \tag{27}$$

So

$$\begin{aligned} r_x &= \frac{x}{r} \qquad r_y = \frac{y}{r} \qquad r_z = \frac{z}{r} \\ \theta_x &= -\frac{y}{x^2+y^2} \qquad \theta_y = \frac{x}{x^2+y^2} \qquad \theta_z = 0 \\ \phi_x &= \frac{xz}{r^2\sqrt{x^2+y^2}} \qquad \phi_y = \frac{yz}{r^2\sqrt{x^2+y^2}} \qquad \phi_z = -\frac{\sqrt{x^2+y^2}}{r^2} \end{aligned} \tag{28}$$

The solution to the wave equation has an expansion

$$p(t,r,\theta,\phi) = \sum_{j=1}^{j=\infty} \frac{f_j(ct-r,\theta,\phi)}{r^j}$$

We recall that the velocities can be expressed in terms of the divergence and curl of potentials (13) and these potentials solve a wave equation (16). Let $\overrightarrow{u} = (u,v,w)$ be the Cartesian components of the velocity then we have

$$\overrightarrow{u} = \sum_{j=1}^{j=\infty} grad(\frac{f_j(c_p t-r,\theta,\phi)}{r^j}) + \sum_{j=1}^{j=\infty} curl(\frac{\overrightarrow{g_j}(c_s t-r,\theta,\phi)}{r^j}) \tag{29}$$

We write explicitly the first term of the series with $\overrightarrow{g_1} = (g_{11}, g_{12}, g_{13})$. Let (u,v,w) be the Cartesian components of the velocity. Then

$$\begin{aligned} u &= \frac{\partial(\frac{f_1}{r})}{\partial x} + \frac{\partial(\frac{g_{13}}{r})}{\partial y} - \frac{\partial(\frac{g_{12}}{r})}{\partial z} \\ v &= \frac{\partial(\frac{f_1}{r})}{\partial y} + \frac{\partial(\frac{g_{11}}{r})}{\partial z} - \frac{\partial(\frac{g_{13}}{r})}{\partial x} \\ w &= \frac{\partial(\frac{f_1}{r})}{\partial z} + \frac{\partial(\frac{g_{12}}{r})}{\partial x} - \frac{\partial(\frac{g_{11}}{r})}{\partial y} \end{aligned} \tag{30}$$

We next convert the Cartesian derivatives to spherical derivatives. We emphasize that we have spherical derivatives of the Cartesian components, To convert from Cartesian derivatives to spherical derivatives we have

$$\begin{aligned} \frac{\partial}{\partial x} &= \cos(\theta)\sin(\phi)\frac{\partial}{\partial r} - \frac{\sin(\theta)}{r\sin(\phi)}\frac{\partial}{\partial \theta} + \frac{\cos(\theta)\cos(\phi)}{r}\frac{\partial}{\partial \phi} \\ \frac{\partial}{\partial y} &= \sin(\theta)\sin(\phi)\frac{\partial}{\partial r} + \frac{\cos(\theta)}{r\sin(\phi)}\frac{\partial}{\partial \theta} + \frac{\sin(\theta)\cos(\phi)}{r}\frac{\partial}{\partial \phi} \\ \frac{\partial}{\partial z} &= \cos(\phi)\frac{\partial}{\partial r} - \frac{\sin(\theta)}{r}\frac{\partial}{\partial \phi} \end{aligned}$$

We denote by f' the derivative of $f(ct-r,\theta,\phi)$ with respect to the first argument. For ease we shall drop the subscript 1 for f and the first subscript of g,

$$\begin{aligned} u &= -\frac{1}{r}\left(\cos(\theta)\sin(\phi)f' + \sin(\theta)\sin(\phi)g_3' - \cos(\phi)g_2'\right) + O(\frac{1}{r^2}) \\ v &= -\frac{1}{r}\left(\sin(\theta)\sin(\phi)f' + \cos(\phi)g_1' - \cos(\theta)\sin(\phi)g_3'\right) + O(\frac{1}{r^2}) \\ w &= -\frac{1}{r}\left(\cos(\phi)f' + \cos(\theta)\sin(\phi)g_2' - \sin(\theta)\sin(\phi)g_1'\right) + O(\frac{1}{r^2}) \end{aligned} \tag{31}$$

Therefore,

$$
\begin{aligned}
u_t + c_p u_r + \frac{u}{r} &= \frac{1}{r}(c_p - c_s)\left(\sin(\theta)\sin(\phi)g_3'' - \cos(\phi)g_2''\right) \\
u_t + c_s u_r + \frac{u}{r} &= -\frac{1}{r}(c_p - c_s)\cos(\theta)\sin(\phi)f'' \\
v_t + c_p v_r + \frac{v}{r} &= \frac{1}{r}(c_p - c_s)\left(\cos(\phi)g_1'' - \cos(\theta)\sin(\phi)g_3''\right) \\
v_t + c_s v_r + \frac{v}{r} &= -\frac{1}{r}(c_p - c_s)\sin(\theta)\sin(\phi)f'' \\
w_t + c_p w_r + \frac{w}{r} &= \frac{\sin(\phi)}{r}(c_p - c_s)\left(\cos(\theta)g_2'' - \sin(\theta)g_1''\right) \\
w_t + c_s w_r + \frac{w}{r} &= -\frac{1}{r}(c_p - c_s)\cos(\phi)f''
\end{aligned}
\tag{32}
$$

We can then take combinations of these equations to eliminate the right hand sides. We therefore, arrive at the following ABCs

$$
\begin{aligned}
&\cos(\phi)\left[w_t + c_p w_r\right] + \sin(\phi)\left[\cos(\theta)(u_t + c_s u_r + \frac{u}{r}) + \sin(\theta)(v_t + c_p v_r + \frac{v}{r})\right] = 0 \\
&\sin(\theta)(u_t + c_p u_r) - \cos(\theta)(v_t + c_s v_r + \frac{v}{r}) = 0 \\
&\cos(\phi)(u_t + c_p u_r) - \cos(\theta)\sin(\phi)(w_t + c_s w_r + \frac{w}{r}) = 0
\end{aligned}
\tag{33}
$$

6 Stress-Velocity Formulation

From (5) we ignore the x and y derivatives. This yields

$$\rho u_t = \tau_{13z} \quad \tau_{13t} = \rho c_s^2 u_z \tag{34a}$$
$$\rho v_t = \tau_{23z} \quad \tau_{23t} = \rho c_s^2 v_z \tag{34b}$$
$$\rho w_t = \tau_{33z} \quad \tau_{33t} = \rho c_p^2 w_z \tag{34c}$$
$$\tau_{11t} = \lambda w_z \tag{34d}$$
$$\tau_{22t} = \lambda w_z \tag{34e}$$
$$\tau_{12t} = 0 \tag{34f}$$

Note, that the first three lines each form a decoupled set of two equations. c_s is a double eigenvalue, c_p is a single eigenvalue and zero is a triple eigenvalue. The eigenvectors corresponding to c_s are $u \pm \frac{1}{\rho c_s}\tau_{13}$ and $v \pm \frac{1}{\rho c_s}\tau_{23}$ while the eigenvectors corresponding to c_p are $w \pm \frac{1}{\rho c_p}\tau_{33}$. These are exactly the expressions that appear in the Lysmer–Kuhlemeyer ABC (12).

Thus, at the top we must specify three boundary conditions corresponding to the incoming waves. The three zero eigenvalues do not determine if a boundary condition is required. Instead of the Lysmer–Kuhlemeyer ABC we can use the more general ABC (21) that we have discussed. We use the first order elastic equations (5) to eliminate the terms u_x and w_x in (21). This results in:

$$
\begin{aligned}
(\tau_{13})_t &= \rho c_s u_t - \rho c_s(\beta - c_s)w_x \\
(\tau_{23})_t &= \rho c_s v_t - \rho c_s(\beta - c_s)w_y \\
(\tau_{33})_t &= \frac{\lambda}{\alpha}w_t + c_p(\rho c_p - \frac{\lambda}{\alpha})w_z \qquad \lambda = \rho(c_p^2 - 2c_s^2).
\end{aligned}
\tag{35}
$$

As before, $\alpha = \frac{\lambda}{\rho c_p}$ and $\beta = c_s$ recovers the Petersson–Sjögreen / Lysmer–Kuhlemeyer ABC while choosing $\alpha = \beta = c_p - c_s$ (i.e. $\beta - c_s = c_p - 2c_s$) yields Stacey's formula.

In addition, we have three waves that correspond to a zero eigenvalue, i.e. they contain no normal, z, derivatives. These are given by

$$\begin{aligned} \tau_{12t} &= \mu(u_y + v_x) \\ \tau_{11t} - \tau_{22t} &= (\rho c_p^2 - \lambda)(u_x - v_y) \\ \rho c_p^2 \tau_{11t} - \lambda \tau_{33t} &= (\rho c_p^2 - \lambda)\left((\rho c_p^2 + \lambda)u_x + \lambda v_y\right) \\ &= 2\rho^2 c_s^2 \left(2(c_p^2 - c_s^2)u_x + (c_p^2 - 2c_s^2)v_y\right). \end{aligned} \tag{36}$$

7 Higher Order and Frequency Domain

In this section we consider both second order ABCs and extensions to the frequency domain. Stacey presents a second order ABC (his scheme P5) as:

$$\begin{aligned} u_{zt} &= -c_s u_{zz} + \frac{c_p - c_s}{c_p - 2c_s}(w_{xt} + 2c_s w_{xz}) + \frac{c_p c_s}{c_p - 2c_s} u_{xx} \\ w_{zt} &= -c_p w_{zz} - \frac{c_p - c_s}{2c_p - c_s}(u_{xt} + 2c_p u_{xz}) - \frac{c_p c_s}{2c_p - c_s} w_{xx}. \end{aligned} \tag{37}$$

We now use the elastic wave equation (4) to replace u_{zz} and w_{zz} by time derivatives. We shall do this twice once when we completely remove the zz derivatives and once where we replace half the zz derivatives; each approach has its advantage.

We first eliminate the zz derivatives in (37) using the elastic wave equation (4). This results in

$$\begin{aligned} u_{tt} + c_s u_{zt} - \frac{c_s(c_p - c_s)}{c_p - 2c_s} w_{xt} - \frac{c_p}{2} \frac{(2c_p^2 - 4c_p c_s + c_s^2)}{c_p - 2c_s} u_{xx} - \frac{c_p(c_p - c_s)^2}{c_p - 2c_s} w_{xz} = 0 \\ w_{tt} + c_p w_{zt} + \frac{c_p(c_p - c_s)}{2c_p - c_s} u_{xt} + \frac{c_s}{2} \frac{(2c_s^2 - 4c_p c_s + c_p^2)}{2c_p - c_s} w_{xx} - \frac{c_s(c_p - c_s)^2}{2c_p - c_s} u_{xz} = 0 \end{aligned} \tag{38}$$

This has the form that there is no second normal derivative to the surface. This is an advantage for both finite differences and finite elements. This is especially advantageous for the frequency version, to be presented, where the time differences no longer appear. Stacey notes that there may be problems when $c_p \approx 2c_s$. In addition to the term $c_p - 2c_s$ in the denominator of the second equation the coefficient of u_{xx} and w_{xx} can become zero.

Note: eq. 35 in [43] has an error and the coefficient in U_{xz} in his notation should be $\frac{\beta(\alpha-\beta)^2}{\alpha(2\alpha-\beta)}$.

We next modify (37) by replacing only half of the zz derivatives using (4). This results in

$$\begin{aligned} &u_{tt} + 2c_s u_{zt} - 2\frac{c_s(c_p - c_s)}{c_p - 2c_s} w_{xt} + c_s^2 u_{zz} - c_p \frac{(c_p - c_s)^2}{c_p - 2c_s} u_{xx} \\ &- \frac{(c_p - c_s)(c_p^2 - c_p c_s + 2c_s^2)}{c_p - 2c_s} w_{xz} = 0 \\ &w_{tt} + 2c_p w_{zt} + 2\frac{c_p(c_p - c_s)}{2c_p - c_s} u_{xt} + c_p^2 w_{zz} + c_s \frac{(c_p - c_s)^2}{2c_p - c_s} w_{xx} \\ &+ \frac{(c_p - c_s)(2c_p^2 - c_p c_s + c_s^2)}{2c_p - c_s} u_{xz} = 0 \end{aligned} \tag{39}$$

We write (39) in vector form as a matrix acting on the first order Stacey form (9). So we express (39) as

$$\left(\frac{\partial}{\partial t} - B_2\frac{\partial}{\partial x} - C_2\frac{\partial}{\partial z}\right)\left(\frac{\partial}{\partial t} - B_1\frac{\partial}{\partial x} - C_1\frac{\partial}{\partial z}\right)\begin{pmatrix} u \\ v \end{pmatrix}$$

where

$$B_1 = \begin{pmatrix} 0 & c_p - c_s \\ c_p - c_s & 0 \end{pmatrix} \qquad C_1 = C_2 = \begin{pmatrix} c_s & 0 \\ 0 & c_p \end{pmatrix}$$

$$B_2 = \begin{pmatrix} 0 & -\frac{c_p(c_p-c_s)}{c_p-2c_s} \\ \frac{c_s(c_p-c_s)}{2c_p-c_s} & 0 \end{pmatrix}$$

The term $\left(\frac{\partial}{\partial t} - B_1\frac{\partial}{\partial x} - C_1\frac{\partial}{\partial z}\right)\begin{pmatrix} u \\ v \end{pmatrix} = 0$ is the first order Stacey ABC. Forming higher order ABCs by multiplying a matrix times the previous lower order terms is the procedure used in several sequences of ABCs for the acoustic wave equation e.g. [4], [13]. Thus, it is possible that this approach will lead to local ABCs with an order of accuracy greater than two.

8 Computations

To compare some of the absorbing boundary conditions we consider the three dimensional elastic equations in frequency space. We use our fourth order accurate scheme [21] in stress-velocity variables, see also [6]. The staggering is shown in Fig. 2, which shows a grid sized cube and the positions of the points at which the nine variables are located. These positions are described in the caption.

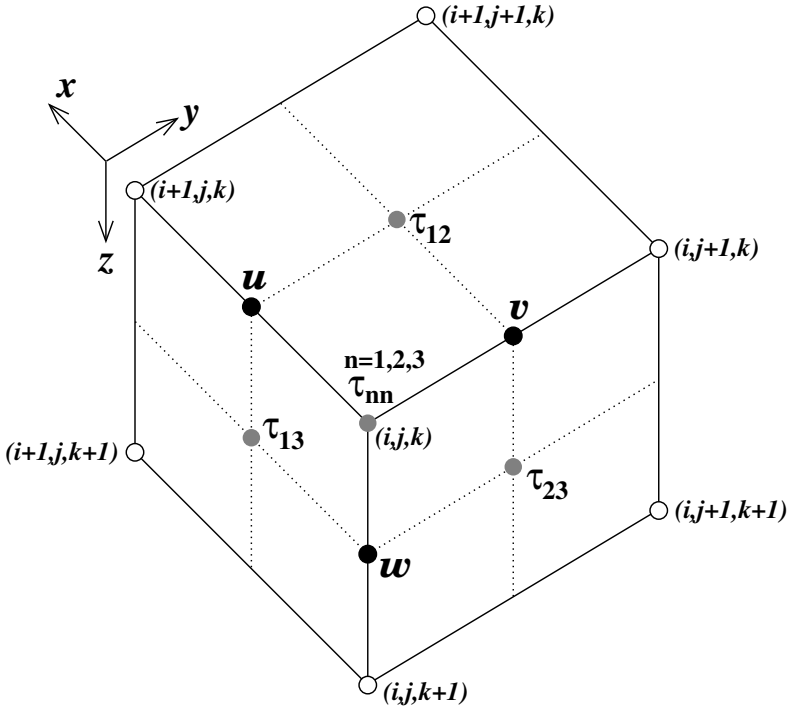

Figure 2: The compact 4th order scheme on a staggered grid, showing the positions of the 9 variables on a cube of 8 adjacent grid points. $\tau_{11}, \tau_{22}, \tau_{33}$ are located at a grid point (i, j, k), u is located at $(i+1/2, j, k)$, v is at $(i, j+1/2, k)$, and w is at $(i, j, k+1/2)$. τ_{12} is at $(i+1/2, j+1/2, k)$, τ_{13} is at $(i+1/2, j, k+1/2)$, and τ_{23} is at $(i, j+1/2, k+1/2)$.

For the elastic wave equation in the frequency domain we replace the time derivative by $i\omega$. By an abuse of notation we denote(u, v, w) as the velocities in frequency space. The first order elastic equations (5) become

$$
\begin{aligned}
i\rho\omega u &= \tau_{11x} + \tau_{12y} + \tau_{13z} + F^u(x, y, z) && \text{(40a)}\\
i\rho\omega v &= \tau_{12x} + \tau_{22y} + \tau_{23z} + F^v(x, y, z) && \text{(40b)}\\
i\rho\omega w &= \tau_{13x} + \tau_{23y} + \tau_{33z} + F^w(x, y, z) && \text{(40c)}\\
i\omega\tau_{11} &= \rho c_p^2 u_x + \lambda(v_y + w_z) && \text{(40d)}\\
i\omega\tau_{22} &= \rho c_p^2 v_y + \lambda(u_x + w_z) && \text{(40e)}\\
i\omega\tau_{33} &= \rho c_p^2 w_z + \lambda(u_x + v_y) && \text{(40f)}\\
i\omega\tau_{12} &= \rho c_s^2(u_y + v_x) && \text{(40g)}\\
i\omega\tau_{13} &= \rho c_s^2(u_z + w_x) && \text{(40h)}\\
i\omega\tau_{23} &= \rho c_s^2(v_z + w_y) && \text{(40i)}
\end{aligned}
$$

Due to the staggering, the variables are not at the same location. Consider the first equation in (40). We center this equation at the position of τ_{13} i.e. at $(i + 1/2, j, k + 1/2)$. u is located at $(i + 1/2, j, k)$ and so we need to average u in the k direction. τ_{13} is at the right location as is w_x. Similarly, the second equation is centered at $(i.j + 1/2, k + 1/2)$ with v averaged in the k direction and the third equation is centered at (i, j, k) with w averaged in the k direction.

The Lysmer and Kuhlemeyer (LK) ABC contains no time derivatives and so remains the same (12) in frequency space. We describe the implementation of the boundary conditions along the absorbing boundary $z = 0$. In (40) we have nine variables and so need nine equations for these variables at or near the boundary. Three are given by the ABC of LK which corresponds to the characteristic variables. Three are given by the variables corresponding to the zero eigenvalues (36). The final three equations correspond to equations from the elastic system.

Thus, the 9 relationships we have at $z=0$ are:

$$
\begin{aligned}
\tau_{13} &= \rho c_s u\\
\tau_{23} &= \rho c_s v\\
\tau_{33} &= \rho c_p w\\
i\omega(\tau_{11} - \tau_{22}) &= (\rho c_p^2 - \lambda)(u_x - v_y)\\
i\omega(\rho c_p^2\tau_{11} - \lambda\tau_{33}) &= 2\mu\left(2(\lambda + \mu)u_x + \lambda v_y\right)\\
i\rho\omega w &= \tau_{13x} + \tau_{23y} + \tau_{33z}\\
i\omega\tau_{12} &= \rho c_s^2(u_y + v_x)\\
i\omega\tau_{13} &= \rho c_s^2(u_z + w_x)\\
i\omega\tau_{23} &= \rho c_s^2(v_z + w_y).
\end{aligned}
\qquad \text{(41)}
$$

The first three equations contain no derivatives but the variables are defined at different locations. Hence, a variable needs to be averaged to get second order accuracy. The last four equations are the same as the original elastic equations and so do not need any averaging. The middle equations involve τ_{nn} which are at the same location. The RHS involves u_x and v_y which centers at the same location and so no averaging is needed. Thus, all the equations can be calculated without using points outside the domain. In summary, averaging is needed only for the LK equations which are the first three equations of (41).

With a different ABC we appropriately replace the first three equations of (41) with an equation that in general will contain the velocities and first derivatives. Thus, for the first order formula of Stacey (9), in

frequency space, we have

$$\begin{aligned} i\omega u &= c_s u_z + (c_p - c_s) w_x \\ i\omega v &= c_s v_z + (c_p - c_s) w_y \\ i\omega w &= c_p w_z + (c_p - c_s)(u_x + v_y). \end{aligned} \tag{42}$$

Each equation contains a z derivative which would require information outside the domain. However, by (40h) we can express u_z in terms of w_x and τ_{13}. Similarly, by (40i) we can express v_z in terms of w_y and τ_{23}. Finally, by (40f) we can express w_z in terms of $u_x + v_y$ and τ_{33}.

We next extend the second order ABC of Stacey to three dimensions in frequency space. Let $s = \sin(\theta)$. Stacey develops (in 2D) a set of equations P5 that has an error $O(s^4)$. Unfortunately, the equations for u and v have a term $c_p - 2c_s$ in some of the denominators. These denominators can be problematic for some Poisson ratios. The lower order ABC P4, which has behaves as $O(s^3)$, does not have this difficulty. Hence, as recommended by Stacey we use P4 for u and v and P5 for w. This yields

$$\begin{aligned} i\omega u &= -c_s u_{zz} - (c_p - c_s)(v_{xy} + w_{xz}) - (c_p - \frac{c_s}{2}) u_{xx} \\ i\omega v &= -c_s v_{zz} - (c_p - c_s)(u_{xy} + w_{yz}) - (c_p - \frac{c_s}{2}) v_{yy} \\ i\omega w_z &= -c_p w_{zz} - \frac{c_p - c_s}{2c_p - c_s} \left(i\omega(u_x + v_y) + 2c_p(u_{xz} + v_{yz}) \right) \\ &\quad - \frac{c_p c_s}{2(2c_p - c_s)} (w_{xx} + w_{yy}). \end{aligned} \tag{43}$$

We again eliminate the normal second derivatives by using the frequency space version of (4). This yields

$$-\omega^2 u + i\omega c_s u - (c_p^2 - c_p c_s + \frac{c_s^2}{2}) u_{xx} - c_s^2 u_{yy} - c_p(c_p - c_s)(w_{xz} + v_{xy}) = 0 \tag{44a}$$

$$-\omega^2 v + i\omega c_s v - (c_p^2 - c_p c_s + \frac{c_s^2}{2}) v_{yy} - c_s^2 v_{xx} - c_p(c_p - c_s)(w_{yz} + u_{xy}) = 0 \tag{44b}$$

$$\begin{aligned} &-\omega^2 w + i\omega c_p \left(w_z + \frac{(c_p - c_s)}{2c_p - c_s}(u_x + v_y) \right) - c_s \frac{(c_p - c_s)^2}{2c_p - c_s}(u_{xz} + v_{yz}) \\ &+ \frac{c_s(c_p^2 + 2c_s^2 - 4c_p c_s)}{2(2c_p - c_s)}(w_{xx} + w_{yy}) = 0. \end{aligned} \tag{44c}$$

We can further eliminate w_z using the frequency version of (5). This gives $i\omega\tau_{33} = \rho c_p^2 w_z + \lambda(u_x + v_y)$ or $w_z = \frac{i\omega\tau_{33} - \lambda(u_x + v_y)}{\rho c_p^2}$. We thus, can calculate all derivatives to second order accuracy without using information outside the domain. Equation (44c) above can then be written as

$$\begin{aligned} &-\omega^2(w + \frac{\tau_{33}}{\rho c_p}) - i\omega \left(\frac{\lambda}{\rho c_p} - \frac{c_p(c_p - c_s)}{2c_p - c_s} \right)(u_x + v_y) - \frac{c_s(c_p - c_s)^2}{2c_p - c_s}(u_{xz} + v_{yz}) \\ &+ \frac{c_s(c_p^2 + 2c_s^2 - 4c_p c_s)}{2(2c_p - c_s)}(w_{xx} + w_{yy}) = 0. \end{aligned} \tag{45}$$

This contains no normal second derivatives. As Stacey notes there are no singularities at $c_p = 2c_s$. However, the equations for u and v have a lower order accuracy than the equation for w.

Equations (44a), (44b) and (45) will be used as ABC on the $z = 0$ boundary. For the $z = 2000$ boundary, we shall also use (44a) and (44b) for u and v, and the following equation for w:

$$\begin{aligned} &-\omega^2(w - \frac{\tau_{33}}{\rho c_p}) + i\omega \left(\frac{\lambda}{\rho c_p} - \frac{c_p(c_p - c_s)}{2c_p - c_s} \right)(u_x + v_y) - \frac{c_s(c_p - c_s)^2}{2c_p - c_s}(u_{xz} + v_{yz}) \\ &+ \frac{c_s(c_p^2 + 2c_s^2 - 4c_p c_s)}{2(2c_p - c_s)}(w_{xx} + w_{yy}) = 0. \end{aligned} \tag{46}$$

For applications, we modify (44) for the $x=0$ boundary as follows:

$$-\omega^2 w + i\omega c_s w - (c_p^2 - c_p c_s + \frac{c_s^2}{2}) w_{zz} - c_s^2 w_{yy} - c_p(c_p - c_s)(u_{xz} + v_{yz}) = 0 \tag{47a}$$

$$-\omega^2 v + i\omega c_s v - (c_p^2 - c_p c_s + \frac{c_s^2}{2}) v_{yy} - c_s^2 v_{zz} - c_p(c_p - c_s)(w_{yz} + u_{xy}) = 0 \tag{47b}$$

$$\begin{aligned} &-\omega^2 u + i\omega c_p \left(u_x + \frac{(c_p - c_s)}{2c_p - c_s}(v_y + w_z) \right) - c_s \frac{(c_p - c_s)^2}{2c_p - c_s}(v_{xy} + w_{xz}) \\ &+ \frac{c_s(c_p^2 + 2c_s^2 - 4c_p c_s)}{2(2c_p - c_s)}(u_{yy} + u_{zz}) = 0. \end{aligned} \tag{47c}$$

Similarly to Eq. (45), we can replace Eq. (47c) with the following equation:

$$\begin{aligned} &-\omega^2(u + \frac{\tau_{11}}{\rho c_p}) - i\omega \left(\frac{\lambda}{\rho c_p} - \frac{c_p(c_p - c_s)}{2c_p - c_s} \right)(v_y + w_z) - \frac{c_s(c_p - c_s)^2}{2c_p - c_s}(v_{xy} + w_{xz}) \\ &+ \frac{c_s(c_p^2 + 2c_s^2 - 4c_p c_s)}{2(2c_p - c_s)}(u_{yy} + u_{zz}) = 0. \end{aligned} \tag{48}$$

Equations (47a), (47b) and (48) will be used as the ABC on the boundary $x = 0$. For the $x = 2000$ boundary, we shall use (47a), (47b), and the following equation for w:

$$\begin{aligned} &-\omega^2(u - \frac{\tau_{11}}{\rho c_p}) + i\omega \left(\frac{\lambda}{\rho c_p} - \frac{c_p(c_p - c_s)}{2c_p - c_s} \right)(v_y + w_z) - \frac{c_s(c_p - c_s)^2}{2c_p - c_s}(v_{xy} + w_{xz}) \\ &+ \frac{c_s(c_p^2 + 2c_s^2 - 4c_p c_s)}{2(2c_p - c_s)}(u_{yy} + u_{zz}) = 0. \end{aligned} \tag{49}$$

We shall now compare two different absorbing boundary conditions, namely, the first and second order Stacey formulae: (42) and (44).

9 Experimental results

9.1 Methodology

In order to evaluate the accuracy of the ABCs given above by (42) and (44),, we will compare results on a problem that has a known analytic solution. The problem (in frequency space) which we consider is a cube of size 2000 meters on all sides, with an impact point at the center in the z direction. The x, y, z axes defining the domain go from zero to 2000. This problem has a known analytic solution — see Pilant [36, Eq. 7-88], Pujol [37, Eq. 9.5.20], and the references therein. The solution presented by Pilant considers a point impact in one direction, was used by [21, 23, 30] and others. The two solutions are mathematically identical, and we chose to use Pujol's solution for this paper.

We present Pujol's formulation of the wave function in 3D, assuming that the impact is in the z-direction, at a point (x_0, y_0, z_0). Let (x, y, z) be the point at which we wish to evaluate the values of u, v, w. We first evaluate the following terms:

$$\alpha = \sqrt{\frac{\lambda + 2\mu}{\rho}}, \qquad \beta = \sqrt{\frac{\mu}{\rho}} \tag{50a}$$

$$r = \sqrt{(x - x_0)^2 + (y - y_0)^2 + (z - z_0)^2} \tag{50b}$$

$$\gamma_1 = \frac{x - x_0}{r}, \quad \gamma_2 = \frac{y - y_0}{r}, \quad \gamma_3 = \frac{z - z_0}{r} \tag{50c}$$

The values of u, v, w at a point (x, y, z) are given by the following:

$$u = \frac{\gamma_1\gamma_3 F(\omega)}{4\pi\rho r}\left[\frac{1}{\alpha^2}e^{-i\omega r/\alpha}\left(1 - \frac{3\alpha}{\omega r}\left(\frac{\alpha}{\omega r} + i\right)\right) - \frac{1}{\beta^2}e^{-i\omega r/\beta}\left(1 - \frac{3\beta}{\omega r}\left(\frac{\beta}{\omega r} + i\right)\right)\right] \tag{51a}$$

$$v = \frac{\gamma_2\gamma_3 F(\omega)}{4\pi\rho r}\left[\frac{1}{\alpha^2}e^{-i\omega r/\alpha}\left(1 - \frac{3\alpha}{\omega r}\left(\frac{\alpha}{\omega r} + i\right)\right) - \frac{1}{\beta^2}e^{-i\omega r/\beta}\left(1 - \frac{3\beta}{\omega r}\left(\frac{\beta}{\omega r} + i\right)\right)\right] \tag{51b}$$

$$w = \frac{F(\omega)}{4\pi\rho r}\left[\frac{1}{\alpha^2}e^{-i\omega r/\alpha}\left(\gamma_3^2 - \left(3\gamma_3^2 - 1\right)\frac{\alpha}{\omega r}\left(\frac{\alpha}{\omega r} + i\right)\right) - \frac{1}{\beta^2}e^{-i\omega r/\beta}\left(\gamma_3^2 - \left(3\gamma_3^2 - 1\right)\frac{\beta}{\omega r}\left(\frac{\beta}{\omega r} + i\right)\right)\right], \tag{51c}$$

where $F(w)$ is the impact force in the z-direction. As noted in [30, p. 1070], the displacements in (51) should be multiplied by $-i\omega$ to obtain the velocities for the frequency domain. $F^w(x_0, y_0, z_0)$ can be taken as a constant, which we assume to be 10^9. Note that since the impact is a single point, the above solution is also the Green's function for the problem.

Our evaluation method consists of calculating the global relative error (rel-err) and various plots showing both the analytic real and the calculated solutions. Rel-err is calculated as follows: if x^* is the true solution and x' is a calculated solution then, rel-err is defined as $\|x^* - x'\|/\|x^*\|$. The real analytic solution is taken from Eq. (51) (after multiplying it by $i\omega$). The error in the calculated solution is due mainly to three factors: the absorbing boundary conditions, the fourth order accuracy of the numerical solution, and the grid spacing. To account for the latter two factors, we shall also compare the following two relative errors: rel-err with an ABC on all sides, and rel-err with Dirichlet BC on all sides.

For the solver, we used the block-parallel CARP-CG algorithm [18], which is a Conjugate Gradient (CG) acceleration of CARP [16]. CARP is a parallel version of the Kaczmarz algorithm [27] for solving linear systems. The CG acceleration of CARP follows the lines of the (non-parallel) CGMN algorithm of Björck and Elfving [8]. CARP-CG is ideally suited for the parallel solution of PDE problems defined over a domain. In previous work, it was found to be very efficient for solving the Helmholtz equation with very high frequencies [19] and convection-dominated PDEs [18] and in general, linear systems with discontinuous coefficients and/or very large off-diagonal elements [17]. It was also used in several previous works, such as [21, 24, 29, 30, 45]. CARP-CG is available from the PHIST toolkit [44]. The mechanism of CARP-CG for solving a PDE over some domain is as follows: the domain is partitioned into subdomains by surfaces passing between grid points. The equations in each subdomain are treated in parallel by separate processors, and the results are unified by averaging the values of borderline grid points. This process is repeated until the residual falls below a given threshold. The proofs of correctness of CARP and CARP-CG appear in [16, 18].

The process of subdividing a domain into subdomains is known as Domain Decomposition (DD). Many papers have been written about the problematic issue of applying DD to the Helmholtz equation; see, for example, Gong et al. [14] and the references therein. The problem occurs at boundaries between subdomains, and even more severely at cross-points, where three or more subdomains meet. In reference [15], it is shown that CARP-CG has no problem at boundaries and cross-points. The reason for this is that in some superspace of the problem space, the subdomain operations and the averaging operations constitute a CG acceleration of the Kaczmarz algorithms. One advantage is that the operations across

boundaries are independent of the problems solved, be they convection-diffusion problems, elastic wave problems, or the Helmholtz equation. Other subdomain methods, such as those in [14] and the references therein, are specific to the Helmholtz equation, and there is no indication that they apply to elasticity or other problems. It is well known that all ABCs are inaccurate for glancing waves parallel to the boundary.

Stacey's first order ABC in frequency space (42) is applied as is on the surface $z = 0$. The explicit solution that we are using is the Pilant/Pujol solution given by (51) which is directed in the z direction. This has the effect that it is grazing along the x and y boundaries which creates difficulties for any ABC. We tried a simple cyclic permutation of u, v, w and the corresponding derivatives, but this produced very poor results, as expected. Hence, for this solution it is necessary to modify the ABC along the x and y boundaries. Note, for a general case where there are no grazing waves a cyclic permutation of the z ABC should work fine. We found that some minor adjustments produced quite good results. For the side $y = 0$, we took the $x = 0$ equations and switched the roles of u and v, and x and y. For the opposite surfaces, the right-hand sides of the corresponding equations were taken as the negation of the respective 0-sides due to the antisymmetry of some of the variables and derivatives. The resulting equations for the six surfaces are the following:

$$\begin{aligned} z{=}0: \quad & i\omega u = c_s u_z + (c_p - c_s) w_x \\ & i\omega v = c_s v_z + (c_p - c_s) w_y \\ & i\omega w = c_p w_z + (c_p - c_s)(u_x + v_y) \end{aligned} \tag{52a}$$

$$\begin{aligned} z{=}2000: \quad & i\omega u = -c_s u_z - (c_p - c_s) w_x \\ & i\omega v = -c_s v_z - (c_p - c_s) w_y \\ & i\omega w = -c_p w_z - (c_p - c_s)(u_x + v_y) \end{aligned} \tag{52b}$$

$$\begin{aligned} x{=}0: \quad & i\omega u = c_p u_x + (c_p - c_s)(v_y + w_z) \\ & i\omega v = c_s v_z + (c_p - c_s) w_y \\ & i\omega w = c_s w_x + (c_p - c_s) u_z \end{aligned} \tag{52c}$$

$$\begin{aligned} x{=}2000: \quad & i\omega u = -c_p u_x - (c_p - c_s)(v_y + w_z) \\ & i\omega v = -c_s v_z - (c_p - c_s) w_y \\ & i\omega w = -c_s w_x - (c_p - c_s) u_z \end{aligned} \tag{52d}$$

$$\begin{aligned} y{=}0: \quad & i\omega u = c_s u_z + (c_p - c_s) w_x \\ & i\omega v = c_p v_y + (c_p - c_s)(u_x + w_z) \\ & i\omega w = c_s w_y + (c_p - c_s) v_z \end{aligned} \tag{52e}$$

$$\begin{aligned} y{=}2000: \quad & i\omega u = -c_s u_z - (c_p - c_s) w_x \\ & i\omega v = -c_p v_y - (c_p - c_s)(u_x + w_z) \\ & i\omega w = -c_s w_y - (c_p - c_s) v_z \end{aligned} \tag{52f}$$

Besides the equations (52), we also apply the last six equations of (40) on the six surfaces to account for the variables τ_{ij}.

The equations for the 8 edges of the surfaces $z = 0$ and $z = 2000$ are identical to the equations of the corresponding z-surface. The equations for the following 3 edges are identical to the y-surface that they belong to: the edge defined by $x = y = 0$, the edge defined by $x = 0$, $y = 2000$, and the edge defined by $x = 2000$, $y = 0$.

This leaves us with the problematic edge defined by $x = y = 2000$, for which none of the above possibilities were satisfactory. We therefore resorted to the second-order ABC of Bayliss, Gunzburger and Turkel [5], denoted BGT2. In [20], it was shown that for the Helmholtz equation, several ABCs with directional derivatives orthogonal to the boundary can be improved very significantly if the directional

derivative is taken in the direction of the *gradient* of the wavefront. In the case of a single point source, the gradient of the wave front and the directional derivative are identical.

In the following definition of BGT2 for the Helmholtz equation, r is the distance from the impact point, and $\boldsymbol{r}$ (boldface) is the vector pointing from the impact point; so $u_{\boldsymbol{r}}$ and $u_{\boldsymbol{rr}}$ are directional derivatives in the direction of $\boldsymbol{r}$.

$$u_{\boldsymbol{rr}} + \left(\frac{4}{r} - 2ik\right) u_{\boldsymbol{r}} + \left(\frac{2}{r^2} - k^2 - \frac{4ik}{r}\right) u = 0 \tag{53}$$

For the elastic wave equation, Eq. (53) was applied to u, v and w. k was replaced by $(k_p + k_s)/2$.

The second order Stacey ABC was applied as follows:

- On the surface $z = 0$, we used equations (44a) and (44b) for u and v, and (45) for w.
- On the surface $z = 2000$, we also used (44a) and (44b) for u and v, and (46) for w.
- On the surface $x = 0$, we used equations (47a) and (47b) for u and v, and (48) for w.
- On the surface $x = 2000$, we also used (47a) and (47b) for u and v, and (49) for w.

In the next section, it will be seen that Stacey's second order ABCs produced worse results than the first order ABCs, so there was no reason to apply it to the $y = 0$ and $y = 2000$ surfaces.

9.2 Numerical results

As mentioned previously, the 2000^3 m^3 cube was divided by a grid of 140^3 grid points. One extra grid point was added to all sides for the boundary conditions. The impact function was simulated by setting a cube of 8^3 grid points at the center of the domain with Dirichlet boundary conditions on the outer surface of the cube, as determined by Eq. (51). Other parameters:

- Wave speeds: $c_p = 5000$ m/s, $c_s = 2500$ m/s;
- Density: $\rho = 1000$ kg/m^3.
- λ and μ are determined by c_p and c_s according to Eq. (2).
- $L = 140$ is the number of grid points per side, and $N = 2000$ is the length of a side of the cube in meters.
- Frequencies used in the experiments: $f = 5, 10, 20$ Hz.
- As mentioned previously, the impact is at the center towards the $z = 10$ plane. The value of the impact, $F(\omega)$ in Eq. (51), is set at 10^9.

In Tables 1–3 below we present the global relative error of w when applying Stacey's first and second order ABCs on some of the sides, at frequencies $f = 5, 10, 20$. In Table 4 we compare the accuracies achieved with Stacey's first order ABC and Dirichlet boundary conditions on all six sides.

Frequency:	$f = 5$	$f = 10$	$f = 20$
Stacey 1st.	0.118	0.126	0.192
Stacey 2nd.	0.234	0.158	0.216

Table 1: Relative error obtained with Stacey 1st. and 2nd. order ABC on the surface $z = 0$, with the Green's function solution.

Below, we present 15 plots of the values of u, v, w along lines parallel to the x, y, z axes, at three different distances from the center, as determined by the i, j, k indices, which vary from 1 to 140 (the grid size).

Frequency:	$f=5$	$f=10$	$f=20$
Stacey 1st.	0.123	0.104	0.155
Stacey 2nd.	0.242	0.201	0.235

Table 2: Relative error with Stacey 1st. and 2nd. order ABC on the surfaces $z = 0$ and $z = 2000$, with the Green's function solution.

Frequency:	$f=5$	$f=10$	$f=20$
Stacey 1st.	0.146	0.158	0.170
Stacey 2nd.	0.593	0.448	0.574

Table 3: Relative error with Stacey 1st. and 2nd. order ABC on the surfaces $x = 0$, $x = 2000$, $z = 0$ and $z = 2000$, with Dirichlet BC on the other sides.

Frequency:	$f=5$	$f=10$	$f=20$
Stacey 1st.	0.172	0.179	0.183
Dirichlet BC	0.0131	0.0335	0.0106

Table 4: Comparison of the relative errors obtained with Stacey 1st. order ABC and Dirichlet BC on all six sides.

i, j, k are the indices along the x, y, z-axes, respectively. The plots show the difference between the calculation with Stacey's 1st. order ABC and the Green's function (which is the true solution). The frequency for these results was set at $f=10$.

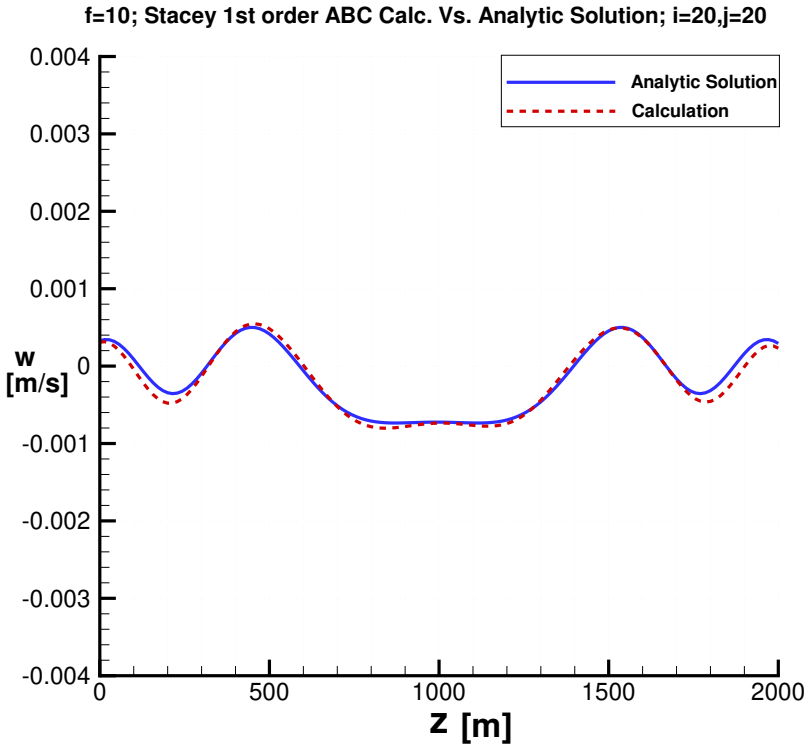

Figure 3: Plot of w parallel to the z-axis, with $i=j=20$.

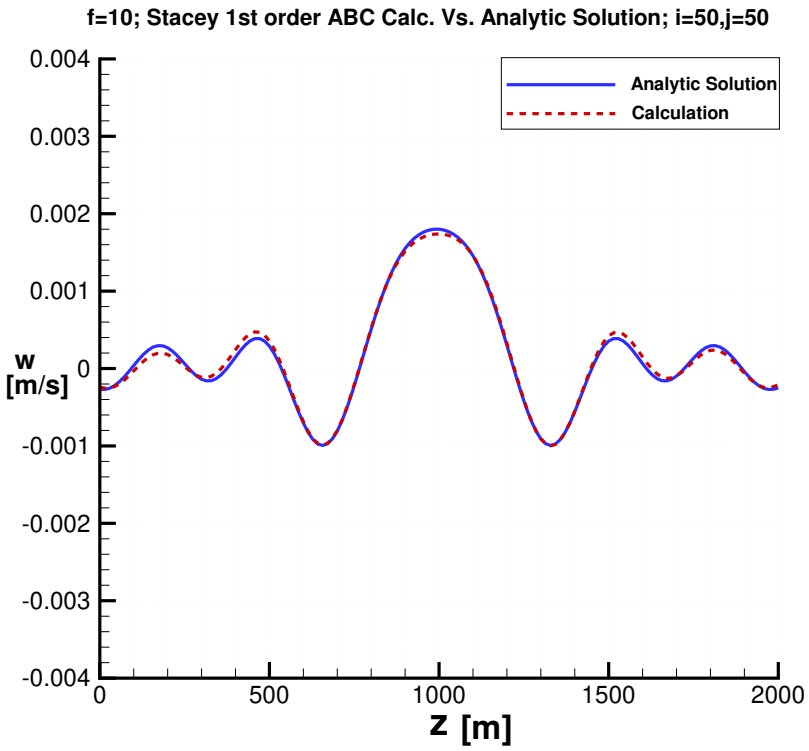

Figure 4: Plot of w parallel to the z-axis, with $i = j = 50$.

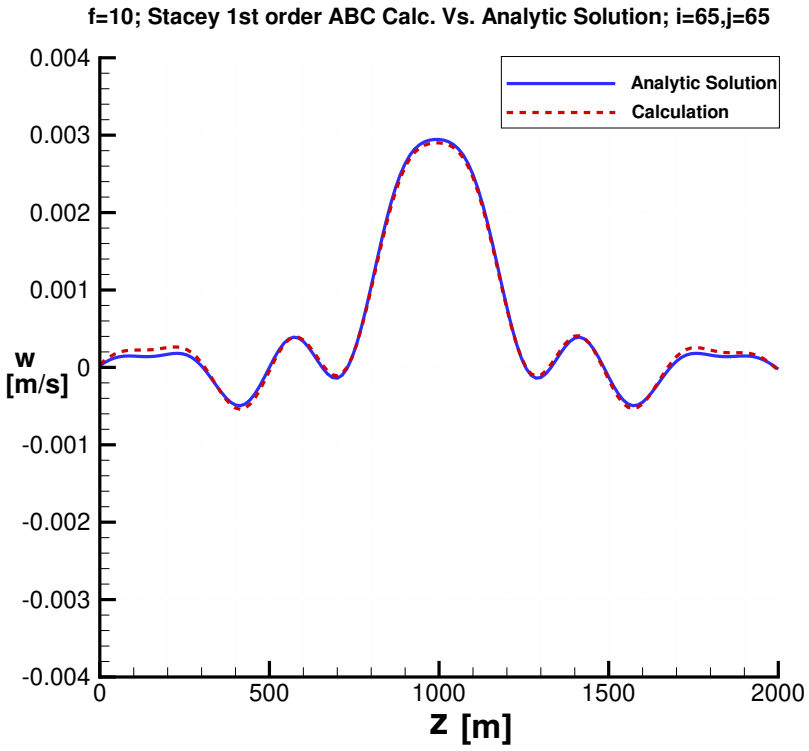

Figure 5: Plot of w parallel to the z-axis, with $i = j = 65$.

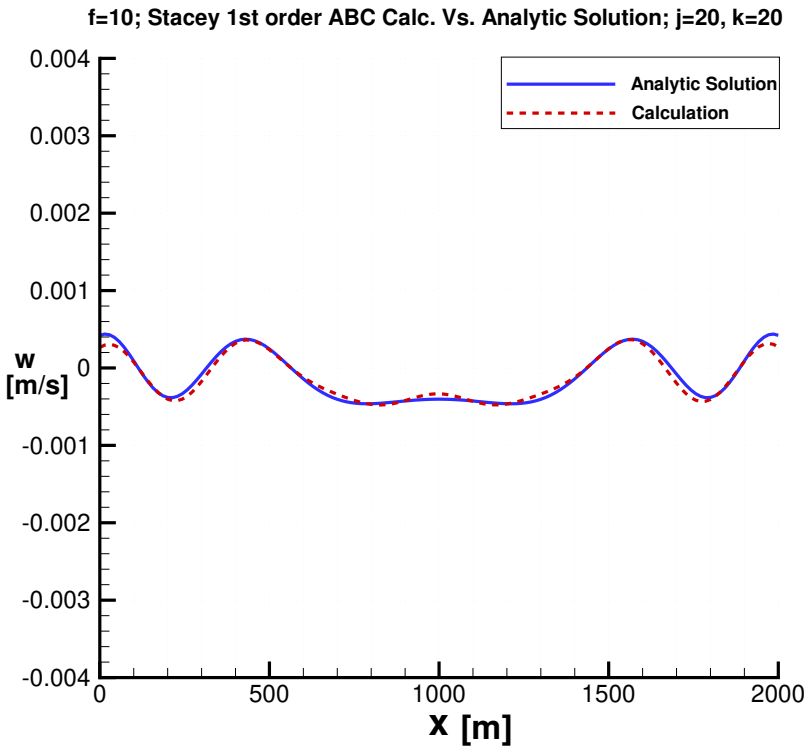

Figure 6: Plot of w parallel to the x-axis, with $j = k = 20$. Note that this plot is identical to that of w parallel to the y-axis.

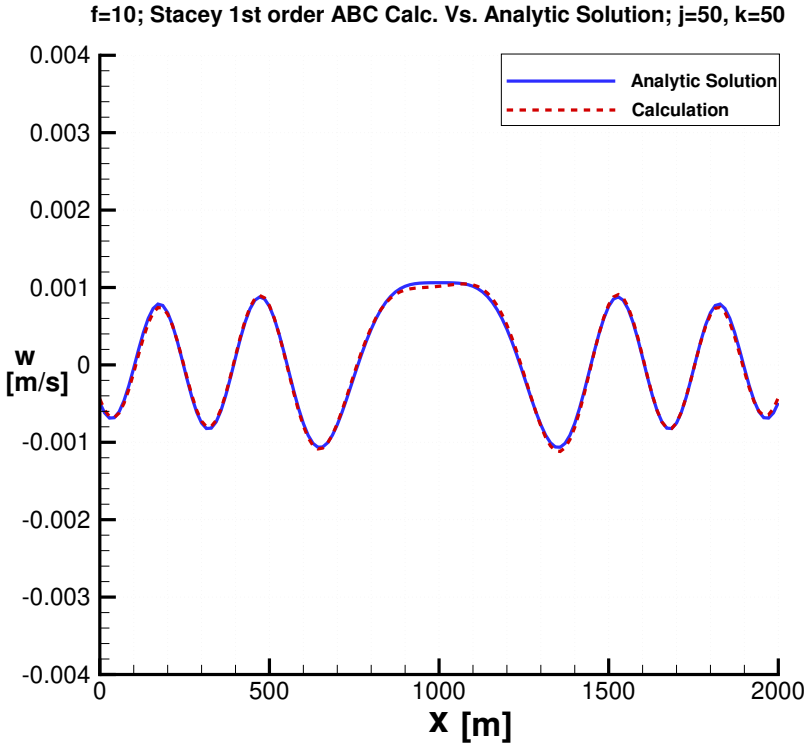

Figure 7: Plot of w parallel to the x-axis, with $j = k = 50$. Note that this plot is identical to that of w parallel to the y-axis.

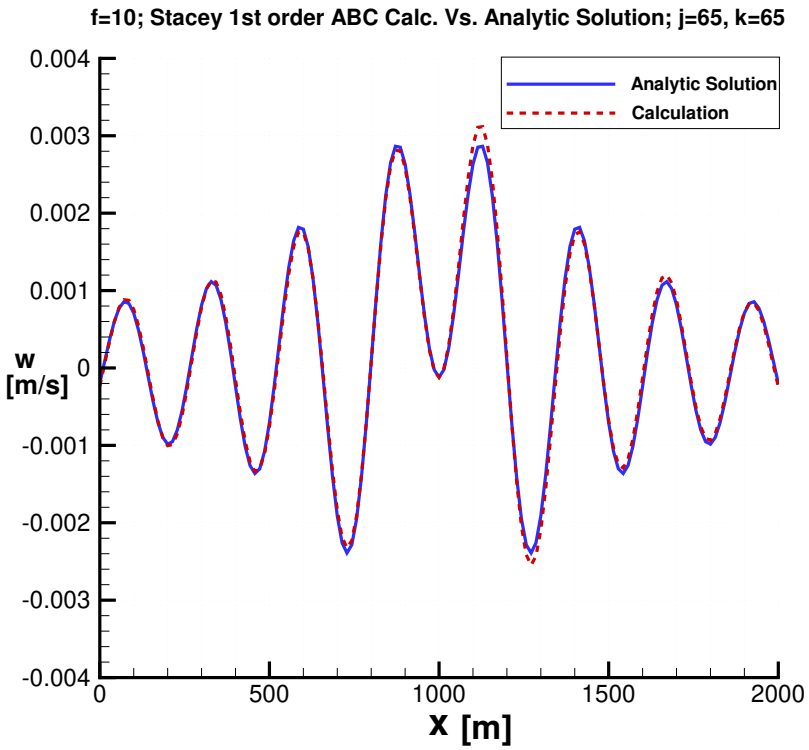

Figure 8: Plot of w parallel to the x-axis, with $j = k = 65$. Note that this plot is identical to that of w parallel to the y-axis.

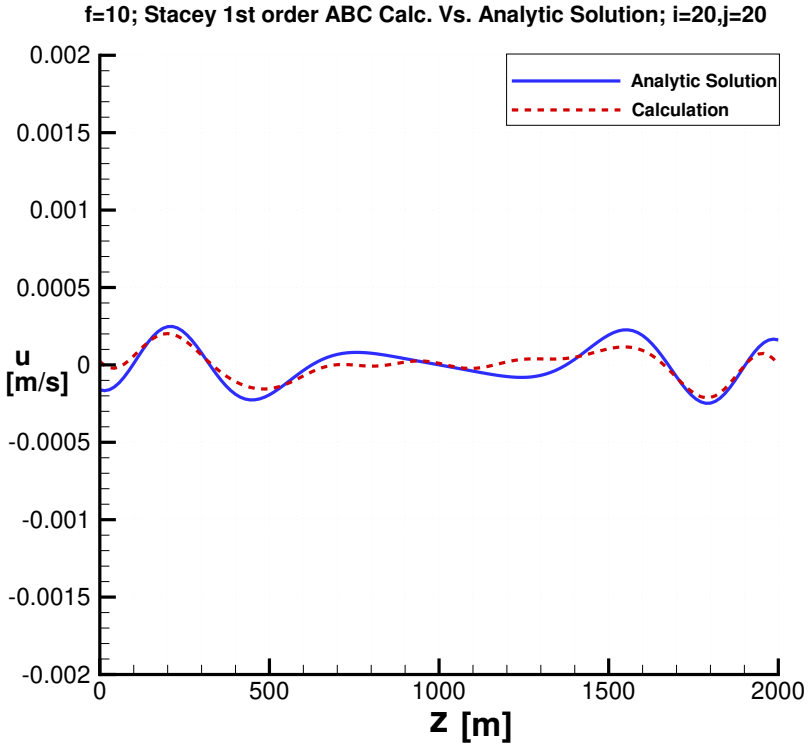

Figure 9: Plot of u parallel to the z-axis, with $i = j = 20$. Note that this plot is identical to that of v parallel to the z-axis.

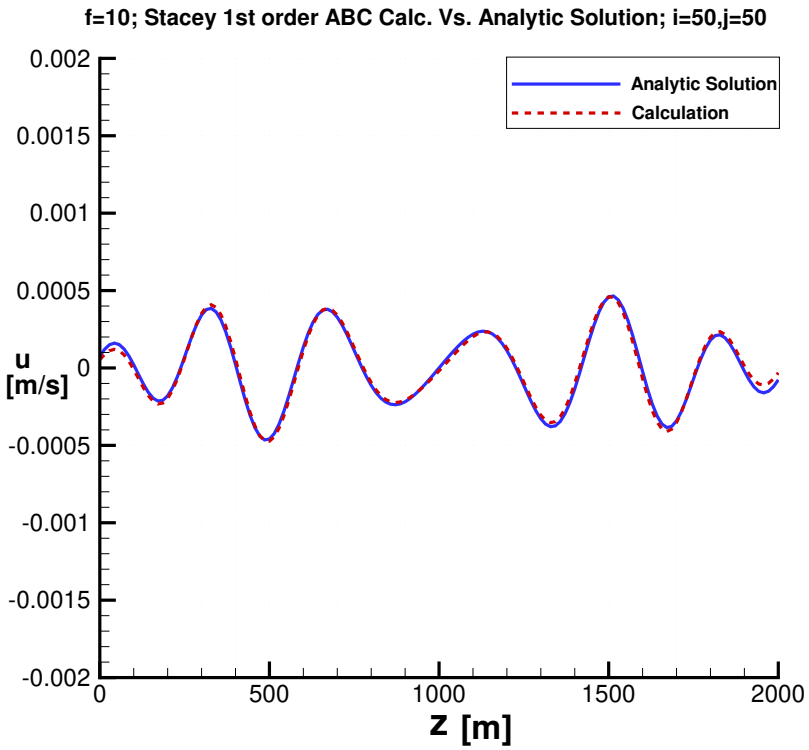

Figure 10: Plot of u parallel to the z-axis, with $i = j = 50$. Note that this plot is identical to that of v parallel to the z-axis.

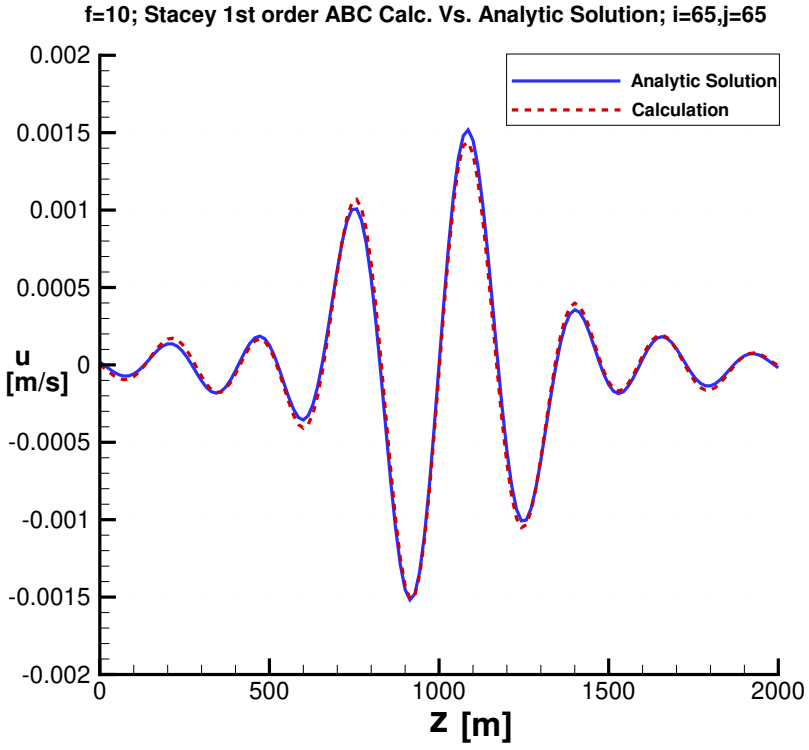

Figure 11: Plot of u parallel to the z-axis, with $i = j = 65$. Note that this plot is identical to that of v parallel to the z-axis.

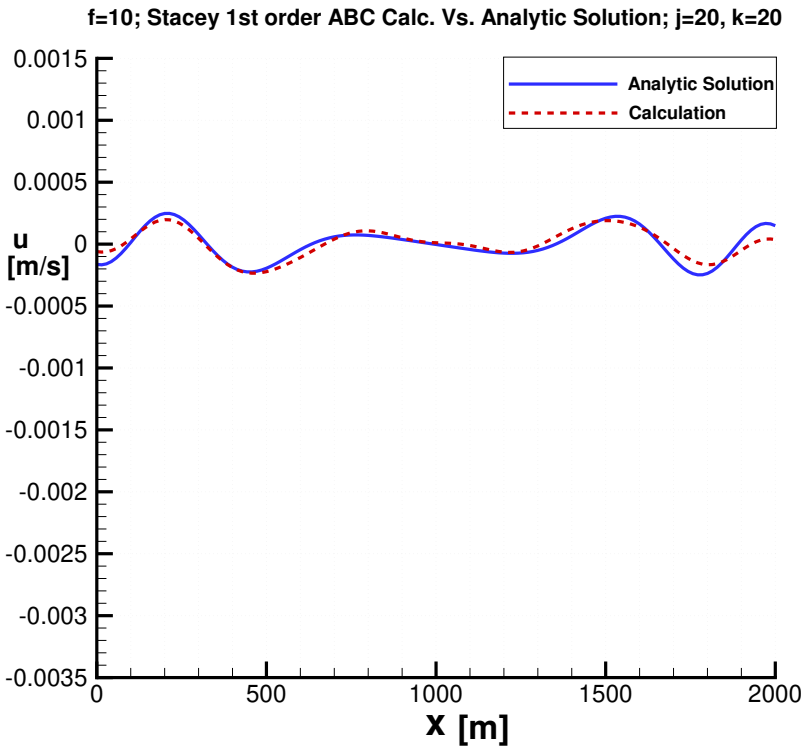

Figure 12: Plot of u parallel to the x-axis, with $j = k = 20$. Note that this plot is identical to that of v parallel to the y-axis.

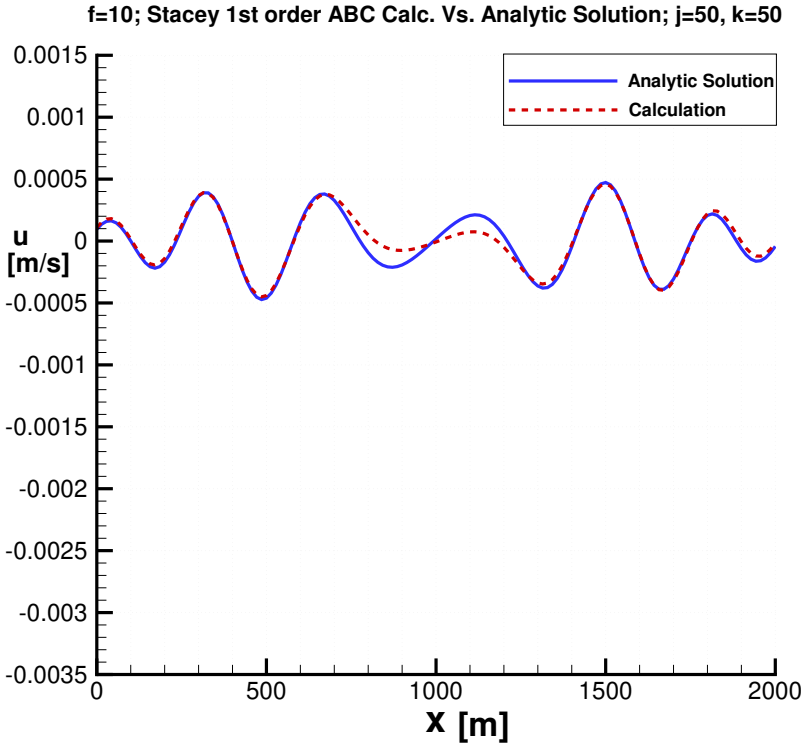

Figure 13: Plot of u parallel to the x-axis, with $j = k = 50$. Note that this plot is identical to that of v parallel to the y-axis.

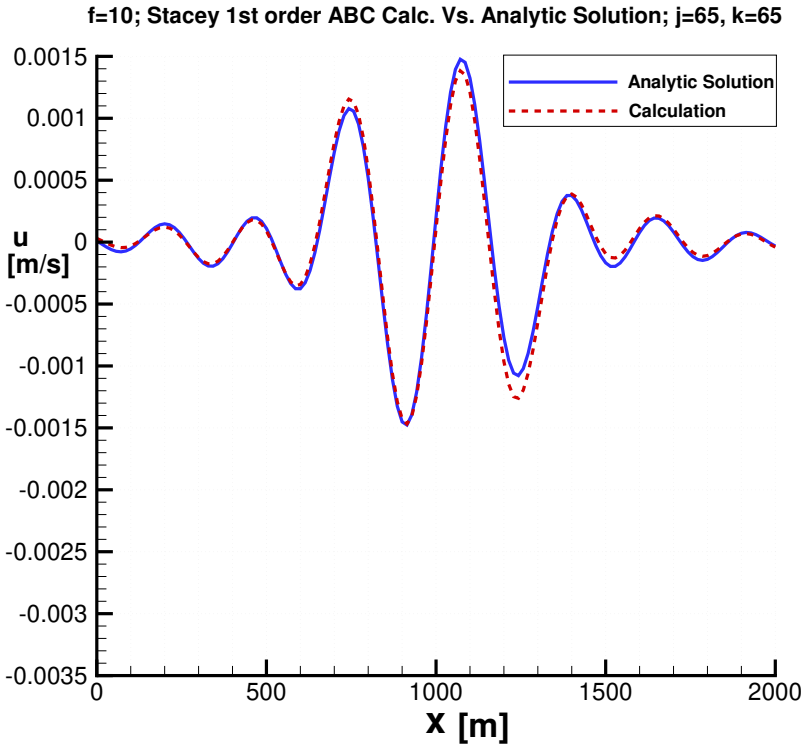

Figure 14: Plot of u parallel to the x-axis, with $j = k = 65$. Note that this plot is identical to that of v parallel to the y-axis.

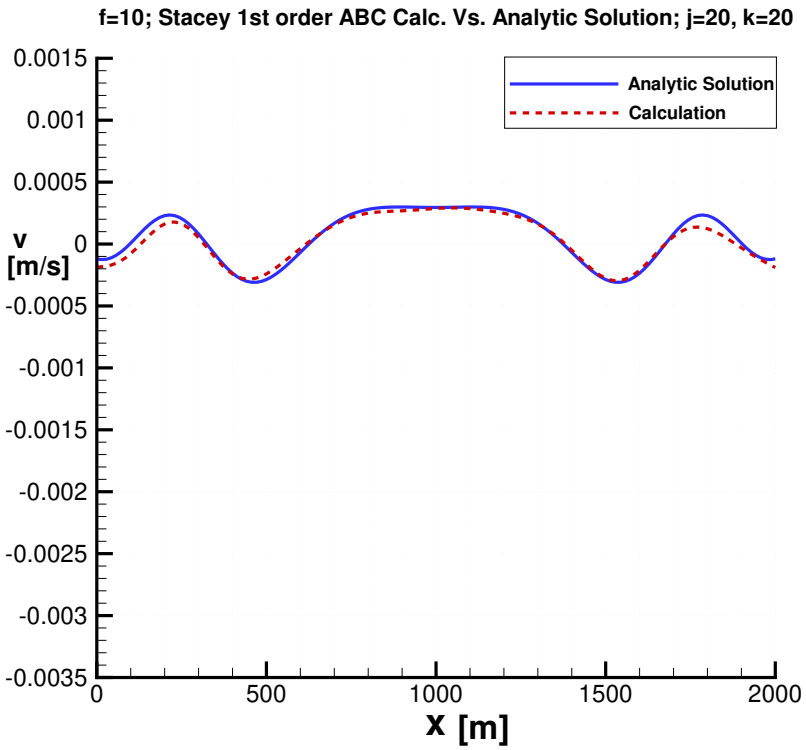

Figure 15: Plot of v parallel to the x-axis, with $j = k = 20$. Note that this plot is identical to that of u parallel to the y-axis.

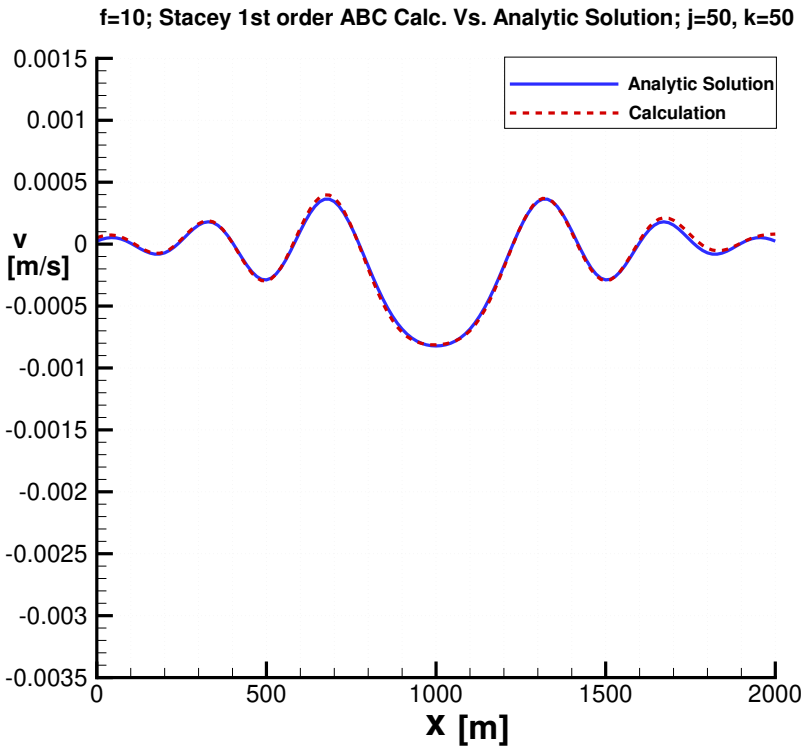

Figure 16: Plot of v parallel to the x-axis, with $j = k = 50$. Note that this plot is identical to that of u parallel to the y-axis.

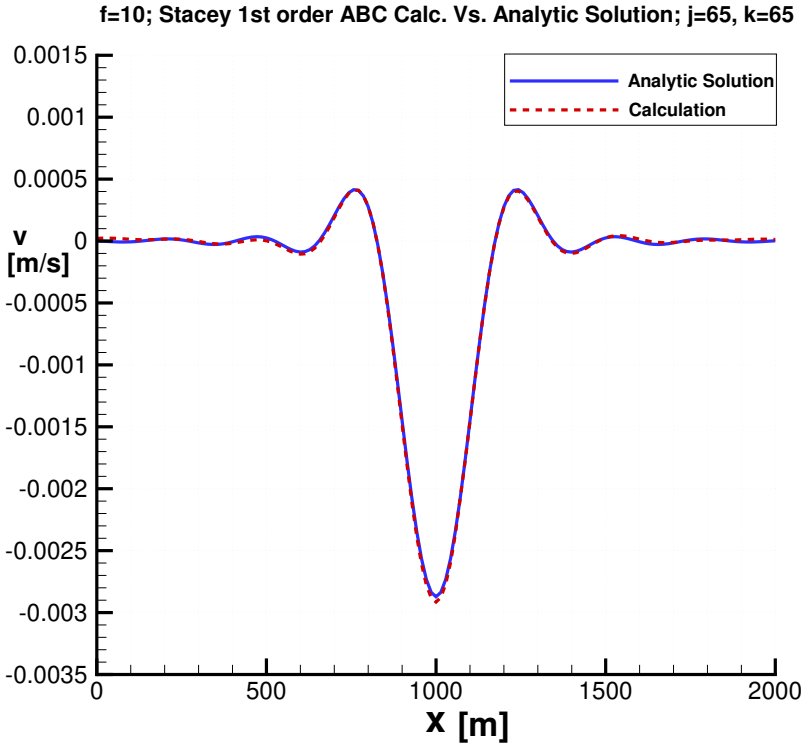

Figure 17: Plot of v parallel to the x-axis, with $j = k = 65$. Note that this plot is identical to that of u parallel to the y-axis.

10 Conclusions

The absorbing boundary condition of Lysmer–Kuhlemeyer is equivalent to that of Petersson–Sjögreen. It is also a set of characteristic variables of the first order system. Of all the first order ABCs of the form (21), only that of Stacey achieves the accuracy $O(\theta^2)$ similar to that which the first order Engquist-Majda achieves for the acoustic wave equation. The second order ABC can be expressed as the multiplication of a new matrix times the first order ABC. A similar formula is derived in spherical coordinates that generalizes the Bayliss–Turkel ABC to the elastic wave equation. Extensions to the first order system and the frequency domain are also presented. Stacey's first order ABC was extended from the $z = 0$ plane to all six surrounding planes, and numerical results show that it achieves good performance, with a global relative error of around 18%. It was also extended to second order, but this extension achieved poor results.

Acknowledgement. The authors are grateful to the reviewers for their helpful suggestions.

References

[1] ABAQUS Theory Manual, Sec. 3.3.1. ABAQUS Inc., Providence, RI, USA. https://classes.engineering.wustl.edu/2009/spring/mase5513/abaqus/docs/v6.6/books/stm/default.htm?startat=ch03s03ath68.html

[2] J.D. Achenbach, *Wave Propagation in Elastic Solids* Elsevier, Amsterdam, 1975.

[3] D. Appelo and T. Colonius. A high order super-grid-scale absorbing layer and its application to linear hyperbolic systems. *J. Comput. Phys.* 228:4200–4217, 2009.

[4] A. Bayliss and E. Turkel. Radiation boundary conditions of wave-like equations. *Comm. Pure Appl. Math.* 33:707–725, 1980.

[5] A. Bayliss, M. Gunzburger and E. Turkel. Boundary conditions for the numerical solution of elliptic equations in exterior regions. *SIAM J. Appl. Math.* 42: 430–45l, 1982.

[6] A. Bayliss, K. E. Jordan, B. J. LeMesurier and E. Turkel, A Fourth Order Accurate Finite Difference Scheme for the Computation of Elastic Wave, *Bulletin of the Seismological Society*, 76: 1115-1132, 1986.

[7] J.-P. Bérenger. A perfectly matched layer for the absorption of electromagnetic waves. *J. Comput. Physics* 114:185–200, 1994.

[8] Å. Björck and T. Elfving. Accelerated projection methods for computing pseudoinverse solutions of systems of linear equations. *BIT* 19:145–163, 1979.

[9] R. Clayton and B. Engquist. Absorbing boundary conditions for acoustic and elastic wave equations. *Bull. Seis. Soc. America* 67(6):1529–1540, 1977.

[10] M. Cohen. PhD thesis, *Silent Boundary Methods for Transient Wave Analysis* California Institute of Technology, Pasadena CA, 1981.

[11] M. Cohen and P.C. Jennings. Silent boundary methods for transient analysis. In: *Computational Methods for Transient Analysis*, T. Belytschko and T.J.R. Hughes, editors, Elsevier, Amsterdam, 301–357, 1983.

[12] A. Ditkowski, M. Sever. On the intersection of sets of incoming and outgoing waves. *Quart. Appl. Math.* 66:1–26, 2008.

[13] B. Engquist and A. Majda. Absorbing boundary conditions for the numerical simulation of waves. *Math. Comput.* 31:629–651, 1977.

[14] S. Gong, M.J. Gander, I.G. Graham, D. Lafontaine and E. Spence. Convergence of parallel overlapping domain decomposition methods for the Helmholtz equation. arXiv:2106.05218v2 [math.NA] 16 Jun 2021.

[15] D. Gordon and R. Gordon. CADD:A seamless solution to the Domain Decomposition problem of subdomain boundaries and cross-points. *Wave Motion* 98:102649, Nov. 2020.

[16] D. Gordon and R. Gordon. Component-averaged row projections: a robust, block-parallel scheme for sparse linear systems. *SIAM J. on Scientific Computing* 27:1092–1117, 2005.

[17] D. Gordon and R. Gordon. Solution methods for linear systems with large off-diagonal elements and discontinuous coefficients. *CMES-Computer Modeling in Engineering & Sciences* 53(1):23–45, 2009.

[18] D. Gordon and R. Gordon. CARP-CG: a robust and efficient parallel solver for linear systems, applied to strongly convection dominated PDEs. *Parallel Computing* 36:495–515, 2010.

[19] D. Gordon and R. Gordon. Parallel solution of high frequency Helmholtz equations using high order finite difference schemes. *Applied Mathematics & Computation* 218(21):10737–10754, 2012.

[20] D. Gordon, R. Gordon and E. Turkel. Compact high order schemes with gradient-direction derivatives for absorbing boundary conditions. *J. of Computational Physics* 297:295–315, 2015.

[21] R. Gordon, E. Turkel and D. Gordon. A compact three-dimensional fourth order scheme for elasticity using the first-order formulation. *International J. for Numerical Methods in Engineering* 122:21, Nov. 2021.

[22] F.D. Hastings, J.B. Schneider and S.L. Broschat. Application of the perfectly matched layer (PML) absorbing boundary condition to elastic wave propagation. *J. Acoust. Soc. Am.* 10(5):3061–3069, 1996.

[23] B. Gosselin-Cliche and B. Giroux. 3D frequency-domain finite-difference viscoelastic-wave modeling using weighted average 27-point operators with optimal coefficients. *Geophysics* 79(3):T169–T188, 2014.

[24] Q. He, B. Han, Y. Chen and Y. Li. Application of the finite-difference contrast source inversion method to multiparameter reconstruction using seismic full-waveform data. *J. of Applied Geophysics* 124:4–16, 2016.

[25] R.L. Higdon. Radiation boundary conditions for elastic wave propagation. *SIAM J. Numer. Anal.* 27:831–870, 1990.

[26] R.L. Higdon. Absorbing boundary conditions for acoustic and elastic waves in stratified media. *J. Comput. Phys.* 101(2):386–418, 1992.

[27] S. Kaczmarz. Angenäherte auflösung von systemen linearer gleichungen. *Bulletin de l'Académie Polonaise des Sciences et Lettres* A35:355–357, 1937.

[28] H.S.W. Kim. Finite element analysis with paraxial and viscous boundary conditions for elastic wave propagation. *Engineering* 4:843–849, 2012.

[29] Y. Li, L. Métivier, R. Brossier, B. Han and J. Virieux. 2D and 3D frequency-domain elastic wave modeling in complex media with a parallel iterative solver. *Geophysics* 80(3):T101–T118, 2015.

[30] Y. Li, B. Han, L. Métivier and R. Brossier. Optimal fourth-order staggered-grid finite-difference scheme for 3D frequency-domain viscoelastic wave modeling. *J. of Computational Physics* 321:1055–1078, 2016.

[31] E.L. Lindman Free space boundaries for the scalar wave equatio, *J. of Computational Physics* 18:66–78,1975.

[32] J. Lysmer and R.L. Kuhlemeyer, Finite dynamic model for infinite media. *J. Proc. Amer. Society Civil Engnr.* M4:859–877, 1969.

[33] M. Medvinsky, S. Tsynkov and E. Turkel. Direct implementation of high-order BGT absorbing boundary conditions. *J. Comput, Physics* 376:98–128, 2019.

[34] N.A. Petersson and B. Sjögreen. An energy absorbing far-field boundary condition for the elastic waveequation. *Commun. Comput. Phys.* 6(3):483–508, 2009.

[35] N.A. Petersson and B. Sjögreen. Super-grid modeling of the elastic wave equation in semibounded domains. *Commun. Comput. Phys.* 16:913–955, 2014.

[36] W.L. Pilant. *Elastic Waves in the Earth*. Vol. 11 in *Developments in Solid Earth Geophysics* Series, Elsevier, Holland, 1979.

[37] J. Pujol. *Elastic Wave Propagation and Generation in Seismology*. Cambridge University Press, Cambridge, UK, 2003

[38] D. Rabinovich, D. Givoli, T. Hagstrom and J. Bielak. Stress-velocity complete radiation boundary conditions. *J. Comput. Acous.* 21(3):1350003, 2013.

[39] D. Rabinovich, D. Givoli, J. Bielak and T. Hagstrom. The double absorbing boundary method for a class of anisotropic elastic media. *Comput. Meth. Appl. Mech. Engg.* 315, 2016.

[40] D. Rabinovich, D. Givoli, J. Bielak and E. Turkel. Scatterer identification in a 2D geophysical medium using an augmented computational time reversal method. *Inter. J. Numer. Anal. Meth. Geomechanics*. 45:867-892, 2021.

[41] C.J. Randall. Absorbing boundary condition for the elastic wave equation velocity-stress formulation. *Geophysics* 54(9):1141–1152, 1989.

[42] Y. Shen and V. Giurgiutiu Effective non-reflective boundary for Lamb waves: theory, finite element implementation, and applications. *Wave Motion* 58:22–41, 2015.

[43] R. Stacey. Improved transparent boundary formulations for the elastic-wave equation. *Bull. Seismol. Soc. Amer.* 78(6):2089–2097, 1988.

[44] J. Thies, M. Röhrig-Zöllner, N. Overmars, A. Basermann, D. Ernst, G. Hager and G. Wellein. PHIST: A pipelined, hybrid-parallel iterative solver toolkit. *ACM Trans. on Mathematical Software* 46(4), Oct. 2020.

[45] T. van Leeuwen and F. Herrmann. 3D frequency-domain seismic inversion with controlled sloppiness. *SIAM J. on Scientific Computing* 36(5):S192–S217, 2014.

[46] V. Villamizar, S. Acosta and B. Dastrup. High order local absorbing boundary conditions for acoustic waves in terms of farfield expansions. *J. Comput. Phys.* 333:331—351, 2017.

[47] W.White, S. Valliapan and I.K. Lee. Unified boundary for finite dynamic models. *J. Engng. Mech. Div.* ASCE 103:949–964, 1977.

[48] J. Zhou and N. Saffari. Absorbing boundary conditions for elastic media. *Proc. Royal Society London A* 452:1609–1630, 1996.